Animal Models for Bone Tissue Engineering and Osteoinductive Biomaterial Research

Qifeng Lu, Xiao Lin, and Lei Yang

Abstract Animal bone defect model is the most important and widely used in vivo model for the study of osteoinductive biomaterials and bone tissue engineering. There are many different types of bone defect models at various anatomical sites, including skull and long bones, and using different animals, including mice, rats, rabbits, dogs, swine, and even nonhuman primates. Proper selection of animal model for a specific biomaterial or bone tissue engineering study is critical to obtain reasonable and reliable results. In this chapter, calvarial, weight-bearing long bone segmental defect models, metaphyseal defect models, and vertebral defect models are reviewed referring to several selection criteria of bone defect models. Several issues regarding model selection are discussed, including the characteristics of the model, the material being tested, and the experimental purpose. Considering the inconsistency between the current models and the real clinical conditions, we propose a suggestion for the future development of animal models for bone tissue engineering and osteoinductive biomaterial research.

Keywords Animal model · Bone defect · Fracture · Osteoinductive biomaterials Bone tissue engineering

Qifeng Lu and Xiao Lin contributed equally to this work.

Q. Lu · X. Lin
Orthopaedic Institute and Department of Orthopaedics, The First Affiliated Hospital, Soochow University, Suzhou, Jiangsu, China

L. Yang (✉)
Orthopaedic Institute and Department of Orthopaedics, The First Affiliated Hospital, Soochow University, Suzhou, Jiangsu, China

Center for Health Science and Engineering (CHSE), School of Materials Science and Engineering, Hebei University of Technology, Tianjin, China
e-mail: ylei@hebut.edu.cn

B. Li et al. (eds.), *Racing for the Surface*,
https://doi.org/10.1007/978-3-030-34471-9_11

Introduction

Bone fracture is a common injury. Severe bone fractures are usually comminuted, which may cause bone defects. Nonunion would occur if the size of bone defect is beyond the self-healing ability of bone, which will cause serious pain and medical burden to patients. Furthermore, the repair of bone defects is difficult in clinical treatment due to limited autogenous bone supply.

The development of osteoinductive biomaterials and bone tissue engineering technology brings hope to the treatment of bone defects caused by fracture. For bone defects caused by tumors and osteomyelitis, biomaterials with only osteoinductive capability have limited treatment potential. Thus, this chapter focusses on defects caused by fracture. After development of bioactive bone substitutes, including osteoinductive biomaterials and bone tissue engineering products, evaluation of whether the materials meet the requirements of clinical treatment is necessary. Considering the complexity of the human body, results from in vitro tests cannot properly reflect the performance of biomaterials in vivo. Animal experiments are therefore essential for biomaterial evaluations by simulating the clinical human application.

However, the establishment of a universal animal model applicable to all studies for bone tissue engineering and osteoinductive biomaterial is impossible. A wide variety of bone defect models has been created for testing various materials. The repair of bone defect is affected by many factors, such as stability of the fractured ends of bone, blood supply, infection, and treatment methods, all of which affect the evaluation results of biomaterials. An incorrect selection of model or failure of detail control may seriously affect the results and even mislead the researchers. Therefore, proper animal models should simulate the real conditions of fracture and bone defect well and should be repeatable and standardized to obtain reliable results.

Here, we review the current bone defect models for the researches of osteoinductive biomaterials and bone tissue engineering and provide prospects for the development of defect models, which may serve as a reference for relevant researchers. This review includes three parts. The characteristics and analyses of the each bone defect model are introduced in the first part. The model selection criteria are described and suggested in the second part. Finally, the need for improvement and development of new bone defect models are proposed in the third part.

Animal Bone Defect Models

An ideal animal bone defect model used in osteoinductive biomaterials and bone tissue engineering research needs to meet the following criteria.

Clinical similarity: The animal model should have a similar in vivo environment simulating a specific human disease. For the bone fracture defect model, it should simulate bone defect of human when fracture occurs. Meanwhile, the animal model

should be consistent with the disease severity. In terms of bone defect models, the size of bone defects should exceed the self-repair ability of the body where nonunion occurs without immediate treatment. The smallest size causing nonunion is defined as the critical size defect (CSD) [1]. The CSD values vary with animal model and animal age, weight, defect location, and other pathological factors [2].

Repeatability: Standardized processes and operational methods should be used to produce animal bone defect model, which allows the model to be repeated under the same conditions, rendering the results from the bone defect model reliable and comparable.

There are many types of bone defect models used in the researches of osteoinductive biomaterials and bone tissue engineering. Based on the defect location, the bone defect models can be divided into calvarial bone defect model, long bone segmental defect model, metaphyseal defect model, vertebral body defect model, and long bone multiple defect model, etc. Moreover, each model can be created in different animal species. Within so many kinds of defect model, selecting a suitable model for research is a problem every researcher encounters. Before making choices, an in-depth understanding of these models is necessary.

Calvarial Bone Defect Models

Calvarial bone defects are usually created at the center of parietal bone by using a trephine with a specific diameter after cutting the skin and subcutaneous tissue [7]. This model is easy to create and the procedure is standardized to reach a high repeatability.

CSD in Calvarial Bone Defect Models

The CSD of a mouse skull is 4 mm in diameter for round defects [8]. In addition, bilateral skull defects with 3.5 mm in diameter [7] can be established in one mouse to obtain more reliable results. Table 1 summarizes CSD values for a number of different models.

Calvarial bone defect models are usually created in rats. However, the CSD of cranial bone defects is reported to be approximately 4–8 mm [3, 9–13] (Fig. 1a). Scholars initially recognized that the CSD was 8 mm in diameter [9], which is generally chosen in the level of the dura and sigmoid sinus [9]. However, these large-size cranial defects may damage the sagittal sinus, resulting in increasing the probability of bleeding. Therefore, scholars studied small-size skull defects. Sakata et al. created a 7-mm diameter cranial defect [13]. At 14 days post grafting, no calcified tissue was visible in the defect, and more calcification was seen after 35 days, but this did not fill the calvarial defects [13]. Subsequently, experiments of rat skull defects with diameters of 6, 5, and even 4 mm were reported [12–14]. These small-size bone defect models could make bilateral defects so that it might be used to

Table 1 Calvarial bone defect models for biomaterial evaluations and relevant references

Animal			Bone defect					
Species	Strain and age	Gender	Position	Number	Size	Fixation	Tested biomaterials	Reference
Mouse	LMW transgenic mouse (2 months old)	Male	In central calvarial	Bilateral	3.5 mm in diameter	No	Scaffold (consisting of 70% type 1 collagen and 30% hydroxyapatite) with or without BMP2	L. Xiao [7]
	Nude mouse (8-week-old)	Female	Middle of parietal bone	One	4 mm in diameter (CSD)	No	hACSs co-transduced with Bac-flpo/ Bac-FCBW and Bac-mir148b which seeded into gelatin-coated PLGA scaffolds	Y. Liao [8]
Rat	Rats (mean age 7 months)	Male (365–480 g)	Skull	One	5 mm in diameter (CSD)	No	Mussel powder with or without additional bovine bone graft	D. Rizzo Trotta [3]
	SD rat (adult)	Male	To level of dura and sigmoid sinus	One	8 mm in diameter (CSD)	No	Injectable biopolymer of chitosan and inorganic phosphates was seeded with MSCs and BMP-2	J. Scott [9]
	Fisher-344 rat (12-week-old)	Male	In center of each parietal bone	Bilateral	5 mm in diameter	No	BMP-2 loaded CDHA porous scaffold with sulfated chitosan (SCS)	J. Zhao [10]
	Fischer-344 rat (2-month-old)	–	Skull	One	5 mm in diameter	No	BMP-2 mixed with gelatin gel was crosslinked using Tg	J. Fang [11]
	28-day-old CD strain	Male	Each parietal bone	Two	4 mm in diameter	No	Demineralized bone powder (DBP, 75–250 μm)	J. Glowacki [12]
	Sprague-Dawley (SD) rat (7-week-old males)	–	Skull	One	7 mm in diameter	No	Human mandibular periosteum Cells were cultured three-dimensionally on a collagen sponge	Y. Sakata [13]
	Immunodeficient CBH–ruul/_ nude (8 weeks of age)	Male	Skull	Bilateral	6 mm in diameter	No	CD14 mononuclear cells were induced to differentiate into osteoblast-like cells in combination with biodegradable polymer matrices made from poly-e-caprolactone	H. Chim [14]
	Skeletally mature Sprague-Dawley (7–8 week old)	Athymic, male rats	In the parietal bones	Bilateral	5 mm in diameter	No	Demineralized bone matrix (DBM)	A. Mhawi [15]

	Lewis rat (skeletally mature)	Male	Skull	One	5 mm in diameter	No	Polycaprolactone–tricalcium phosphate (PCL/TCP) scaffolds with two different fiber laydown patterns (coated with hydroxyapatite and gelatin)	A. Berner [17]
Rabbit	New Zealand white (NZW) rabbit (3 months old)	– (about 2.6 kg)	–	One	15 mm in diameter (CSD)	No	The cocultured cells (peripheral blood CD34+ cell) and MSC sheets were also composited with hydroxyapatite	G. Li [4]
	NZW rabbits (6 months old)	– (2.5–3 kg)	–	Four	8 mm in diameter	No	Stromal cell derived factor-1a	X. Liu [5]
	NZW rabbits (5 months old)	Female (3–4 kg)	In the parietal bone	Bilateral	8 mm in diameter (CSD)	No	ASCs were engineered to express the potent osteogenic (BMP-2) or chondrogenic (TGF-β3) factor, seeded into either apatite-coated PLGA or gelatin sponge scaffolds	C. Lin [18]
	NZW rabbits	–	Proximal to coronal suture in parietal bone	Bilateral∗2	8.0 mm in diameter	No	Particulate graft materials with and without P-15, Osteograf with CSP and Osteograf	N. Tovar [19]
Canine	Adult beagle dogs (12–24 months)	Average weight of 23.6 kg	At the parietal bone	Bilateral	20 mm ∗ 20 mm	No	Adipose-derived stem cells (ASCs) and coral scaffold	L. Cui [6]
	Beagle dogs (average 13.3 months)	Male	In bilateral parietal bone	Bilateral	20 mm in diameter (CSD)	No	Disk of OCP/Col (20 mm diameter, 2.5 mm thick) or commercially available sintered porous β-TCP	Y. Tanuma [20]
	Adult mongrel dogs	Male (15–25 kg)	On either side of the external sagittal crest	Bilateral	14 mm trephine defect	No	Implants of bovine bone morphogenetic protein (β-BMP) and a carrier consisting of matrix y-carboxyglutamic acid rich protein	K. Sato [21]
	Beagle dogs (12–13 months old)	Neutered male (average 9.8 kg, 8.6–11.1 kg)	From bregma posteriorly to interfrontal Suture anteriorly	One	3.5 ∗ 3.5 cm	No	0.2 mg/mL rhBMP-2 in absorbable collagen sponge, 0.2 mg/mL rhBMP-2 in absorbable collagen sponge with corticocancellous chips, 0.2 mg/mL rhBMP-2 in absorbable Collagen sponge with mastergraft granules, or 0.4 mg/mL rhBMP-2 in compression resistant matrix carrier	C.R. Kinsella [22]

compare different materials in one single animal, thus improving the reliability of the experiment. The most widely used model is the 5-mm defect model, which is considered to be CSD with bilateral [15, 16] or single defect [3, 11, 17]. With regard to the skull defect with 4-mm diameter, Glowacki et al. [12] found no obvious signs of bone healing even after 6 months of observation. It should be noted that the observation time period for the determination of CSD in the rat skull should be >8 weeks because skull repair is active within the first 4 weeks and essentially stops at the eighth week [15].

For the rabbit calvarial defect model, the CSD is generally considered as a full-thickness defect with a diameter of 15 mm [4] (Fig. 1b). Bilateral bone defects with smaller size were also established on rabbit skull. Lin et al. drilled an 8 mm-

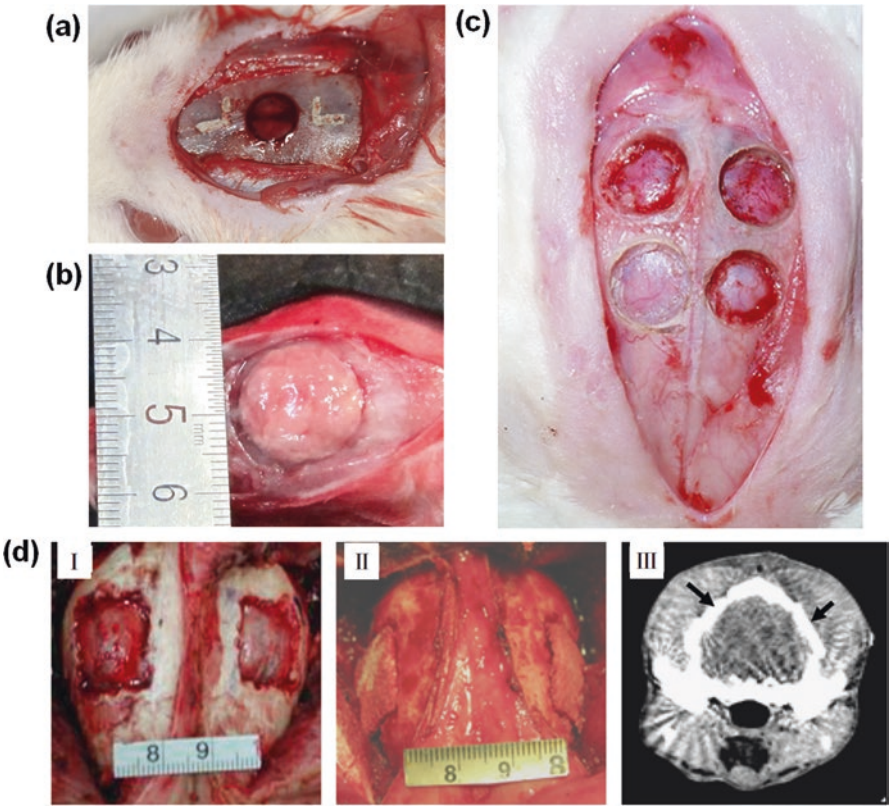

Fig. 1 Calvarial bone defect models: (**a**) a rat calvarial CSD of 5 mm in diameter [3]; (**b**) the composite hydroxyapatite/cell sheet transplanted into the calvarial defect of rabbit (15 mm in diameter) [4]; (**c**) four 8 mm-diameter defects were drilled into the rabbit calvarial bone with a trephine [5]; (**d**) canine calvarial defect model: (I) bilateral full-thickness bone defects with a size of 20 mm × 20 mm were created; (II) the experimental side (left) was repaired with a cell-coral construct and the control side (right) was filled with a coral alone; (III) coronal CT scan image of the same animal was taken immediately after surgery [6]

diameter bilateral full-thickness defect, which was used to compare the repair of bone defect with autologous mesenchymal stem cells (MSCs) [18]. Liu et al. created four 8 mm-diameter defects in the calvarium of rabbits using a trephine attached to a low-speed hand-piece [5] (Fig. 1c). Furthermore, Tovar et al. also drilled two bilateral 8.0 mm-diameter defects without dural injury in the proximal to the coronal suture of the parietal bone [19]. In this way, a variety of bone substitutes have be evaluated by the rabbit calvarial defect model (Table 1).

The CSD in canine skull defect model is usually 20 mm in diameter [20]. With regard to large animal models, making bilateral skull defects is convenient. Sato et al. manufactured bilateral 14-mm trephine defects in dog skull to evaluate the performance of β-sheep bone morphogenetic protein (β-BMP) and a carrier consisting of matrix y-carboxyglutamic acid rich protein [21]. Cui et al. created bilateral full-thickness bone defects with a size of 20 × 20 mm at the parietal bone [6] (Fig. 1d). In addition, a large skull defect area, measuring 35 × 35 mm, was also created in another study [22].

Comments on the Models

Some studies performed periosteal removal in the operative region [12, 23], which might have caused the failure of the skull repair. For example, the stripping of periosteum could even lead to the failure of 2-mm diameter defect healing in rats [24, 25]. Thus, the periosteal layer should be sutured to avoid the obstruction of blood supply when creating animal skull defects.

The operation procedure of the calvarial defect model seems simple, but many things needs special attention to create a successful, repeatable model. The skull is located under the skin; thus, direct skull exposure without intraoperative bleeding is simple. However, prevention of secondary damage is difficult. The surgeon should be careful not to damage the dura mater and the surrounding vessels intraoperatively, or it would cause uncontrollable bleeding. Also, the sagittal sinus may be injured during when creating large-size defects, resulting in obstruction of blood supply. In addition, bone marrow progenitor cells exist in the connective tissue near the sagittal suture, which might be involved in bone remodeling after injury. These factors may critically impact the repair of bone defects.

Segmental Defect Models of Weight-Bearing Long Bone

Weight-bearing bones refer to the bones that bear the main weight of the body in the extremities. The femur and tibia are the most common weight-bearing bones in animal models. The femur size is large, which is convenient for the establishment of bone defect model. And the infection resisting ability of femur model is believed to be strong. However, much muscle tissue around the femur can complicate bone exposure during operation. Because part of tibia is directly under

the skin, tibial exposure is relatively simple, but infection is easy to occur. The selection of model should be based on the purpose of the study and the degree of familiarity of the anatomy.

Fixation Used in the Segmental Defect Model

After the long bone segmental defect forms, the body weight would cause the movement and displacement of the broken ends of the bone, which could affect bone healing and test results. Therefore, internal or external fixation must be used to ensure the stability of defect site.

Rats are often used to create the segmental defect models of weight-bearing long bone. It is however challenging to perform surgery on the slender bones. Kirschner wire is often used for fixing the tibia [30] and femur [31] of rats. However, Kirschner wire in bone marrow cavity occupies much space, causing inconvenience for implanting testing materials. In addition, Kirschner wire has no anti-rotation ability and disturbs the blood supply of defect ends. These shortcomings limit the application of Kirschner wire in the small animal model. Besides the Kirschner wire, external fixator can be used to secure the femoral defect [32, 33], which reveals good anti-rotation ability and preserves the blood supply of defect ends as well as adequate space for implantation. Moreover, the external fixator usually allows animals move freely without the joint being fixed. In recent years, plate fixation [26] (Fig. 2a) and a four-hole high-density polyethylene with stainless-steel screws [34] have been developed for rat femur models. Also, small steel plates and screws have been used to immobilize the femur [35] and tibia [27] (Fig. 2b) of rabbits (Table 2).

With regard to large animals, the weight of the goat and sheep is closer to that of the human body and the size of the bone is also similar to that of the human bones. So more fixation options are available for these animal models. The standard dynamic compression plate (DCP, ten-hole) [36, 37], external fixator [29, 38] (Fig. 2d), screws [28] (Fig. 2c), and internal fixation rods [39, 40] can be used as fixation devices for tibial defects. For femoral defects, internal fixation rods or interlocking nails can be used as fixation devices [39].

CSD in the Segmental Defect Models of Weight-Bearing Long Bone

The CSD of long bone is considered as 1.5–2.5 times the circumference of the diaphysis, or >1/10 of the length [1]. Different animals and bones have different CSDs.

The CSD of the tibia and femur in the rat model are 4 mm [30] and 5 mm [31–34], respectively. For the rabbit model, the CSD of the tibial defect model is determined as 5 mm [27]. However, there are different opinions on the femoral CSD in rabbit models. Fialkov et al. confirmed 12 mm as CSD for femoral diaphyseal defect model [41], but Fan [42] and Duan et al. [35] used a 15-mm defect as CSD.

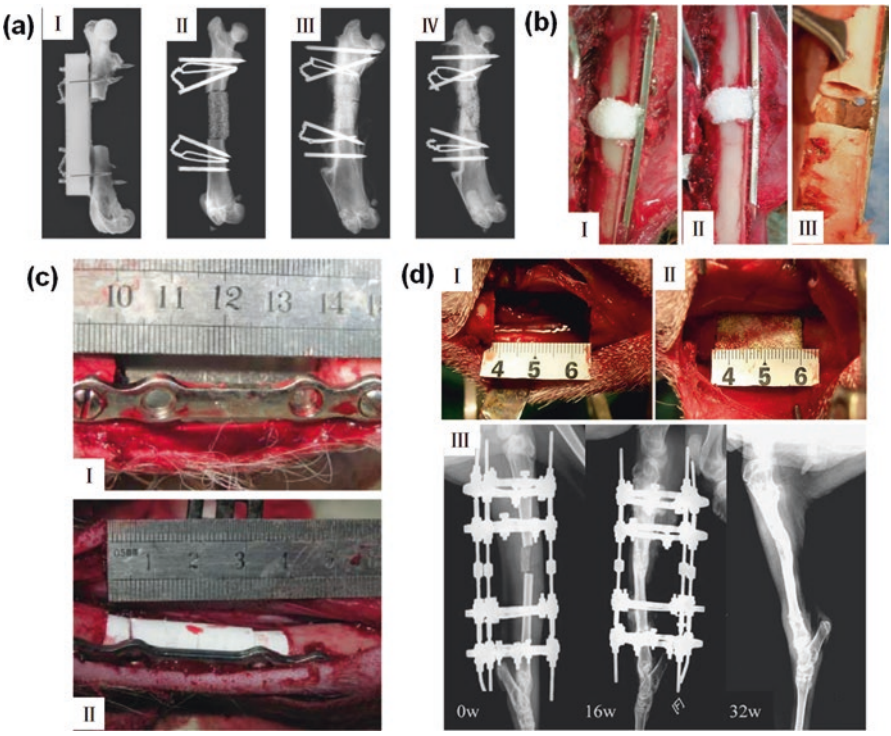

Fig. 2 Weight-bearing long bone segmental defect models with fixations: (**a**) Photo and radiographs of rat femoral defects with fixation (I) prior to implantation, (II) immediately post-implantation, (III) treated with HA/TCP loaded human MSCs at 12 weeks post-implantation, and (IV) treated with HA/TCP alone at 12 weeks post-implantation [26]. (**b**) A 5-mm bone defect was created in the middle of rabbit tibia and stabilized with a plate and screws. The defect was implanted with a complex of β-TCP granules and collagen, either with 200 mg of FGF-2 (I) or without FGF-2 (II). For control group, the bone defect was left empty (III) [27]. (**c**) The 40 mm defect of goat shank with fixation before (I) and after implantation of biomaterial (II) [28]. (**d**) Goat tibia defects model with external fixation. (I) A periosteal segmental defect of 26 mm length was created at the right tibia; (II) the defect was filled with BMSCs/β-TCP construct; (III) radiographs of goat tibial defects taken at different time points post-operation [29]

With regard to large animals, goats and sheep have relatively large limbs that are convenience for modeling surgery using internal fixators. Both the femur and tibia of goat may be used in bone defect models. The segmental defects in the femur is located in the middle of the shaft, and the length of the osteotomy defect could reach up to 25 mm [39]. The sizes of the tibial defect in goats are reported to be different (e.g., 26 mm [38] and 40 mm [28]). For sheep models, the tibia is the most widely used bone and the lengths of defect is either 3.0 cm [36, 37] or 3.5 cm [43], or even 5 cm [40].

Table 2 Weight-bearing long bone segmental defect models for biomaterial evaluations and relevant references

Animal			Bone defect				Experimental biomaterials	Reference
Species	Strain and age	Gender and weight	Position	Number	Size	Fixation		
Rat	Fischer 344 rat	–	Femoral diaphysis	One	8 mm long	Plate fixation	Mesenchymal stem cells (MSCs) combined with biphasic calcium phosphate ceramics	T. L. Livingston [26]
	Wistar albino rat	Female	Central diaphysis of tibia	One	4 mm long	Kirschner wire	RhBMP-2-containing absorbable collagen sponges	S. Sarban [30]
	Brown Norway rat (13 week old)	–	Femoral diaphysis	One	5 mm long	Kirschner wire	Biodegradable polypropylene Fumarate/tricalcium phosphate (PPF/TCP) with dicalcium phosphate dihydrate (DCPD) cement portals	R. Stewart [31]
	–	–	Midfemoral	One	5 mm long (CSD)	External fixator	11 mg of recombinant human BMP (rhBMP)-2 on a collagen sponge	V. Glatt [32]
	Wistar rat (9–11 weeks old)	– (350–440 g)	Mid-diaphyseal femur	One	5 mm long	External fixation	Combined poly (ethylene glycol) diacrylate (PEGDA) hydrogel with allogeneic “carrier” cells transduced with an adenovirus expressing BMP2	C. Sonnet [33]
	SD rat	Male (325–360 g)	Mid-diaphyseal femoral	One	5 mm long	Four-hole high-density polyethylene custom fabricated internal fixator	Recombinant human bone morphogenetic protein-2 (rhBMP-2) absorbable collagen Sponges carrying rhBMP-2	S.R. Angle [34]
Rabbit	NZW rabbit	Female (3.3–3.5 kg)	In middle of tibial diaphysis	Unilateral	5 mm long	A plate and four screws	A complex of β-tricalcium phosphate (β-TCP) granules, collagen, and fibroblast growth factor-2 (FGF-2)	H. Komaki 2006 [27]

	NZW rabbit (16–20 weeks old)		Femoral diaphysis	Unilateral	15 mm long	Five hole steel plates	BMP2-derived peptide Plus PLGA-[ASP-PEG] scaffold material	Z. Duan 2008 [35]
	NZW rabbit	Female (2.0–2.5 kg)	Femoral diaphysis	Unilateral	1.2 cm long	A 2.7-mm mandibular reconstruction plate fixated with three screws on either side of the osteotomy site	A biodegradable scaffold-poly(lactide-*co*-glycolide) (PLGA) foam-with similar porosity to human trabecular bone	J.A. Fialkov [41]
	New Zealand rabbit	Male (2–2.5 kg)	Femoral diaphysis between the second and the third holes of the plate	Unilateral	1.5 cm long	A four-hole steel plate of reconstruction	Tissue-engineered bone and implanted the sensory nerve tracts, blood vessel, or nothing	J.J. Fan [42]
Sheep	Merino sheep (7–8 years)	Average 43.3 kg	Mid-diaphyseal tibia	Unilateral	3 cm long (CSD)	A ten-hole, stainless steel, dynamic compression plate (DCP)	Two dosages of rhBMP-7, 3.5 mg and 1.75 mg, embedded in a slowly degradable medical grade poly(ε-caprolactone) (PCL) scaffold with β-tricalcium phosphate microparticles (Mpcl-TCP)	A. Cipitria [36]
	Merino sheep (6–7 years)	45 ± 2 kg	Mid-diaphyseal tibia	Unilateral	3 cm long (CSD)	A broad dynamic compression plate (DCP) (4.5 mm, ten holes, synthes)	Allogenic mpcs	A. Berner [37]
	Skeletally mature ewes	Female	Mid-diaphyseal tibia	Unilateral	5 cm long (CSD)	An intramedullary interlocking nail with two 4.5 mm cortical	The standard osteogenic protein-1 (OP-1/BMP-7) implant with carboxymethylcellulose (CMC)	G. E. Pluhar [40]

(continued)

Table 2 (continued)

Animal			Bone defect				Experimental bio materials	Reference
Species	Strain and age	Gender and weight	Position	Number	Size	Fixation		
	Sheep (2 years old)	Female	Mid-diaphyseal tibia	Unilateral	3.5 cm long	4.5 mm transcortical screws, four proximal screws, and four distal screws	Blood-derived progenitor cells that have endothelial characteristics (EPC)	N. Rozen [43]
Goat	Adult male goat	About 50 kg	Mid-diaphyseal tibia	Unilateral	40 mm long	A titanium screw	A novel nanohydroxyapatite/collagen/PLLA (nhacp) composite reinforced by chitin fibers	X. Li [28]
	Skeletally mature goat	22.3 ± 4.1 kg	Tibial diaphysis	One	26 mm long	External fixators	Bone marrow stromal cells and ß-tricalcium phosphate	G. Liu [29]
	Goat (1-year-old)	18.6–31.5 kg	Mid-diaphyseal tibia	Unilateral	2.6 cm long	Circular external fixators	Biphasic calcined bone (BCB) and autologous bone marrow-derived mesenchymal stem cells (BMSCs) transduced with human bone morphogenetic protein-2 (hBMP-2)	K. R. Dai 2005 [38]
	Adult goat (12–14 months)	16.5–23 kg (average of 19.6 kg)	Mid-diaphyseal femur	One	25 mm long	An internal fixation rod and interlocking nails	Coral cylinder alone, or filled with coral cylinder plus induced BMSCs	L. Zhu [39]
	Ewe (2-year-old)	–	Tibial diaphysis	One	35 mm long	External fixation	Large, cylindrical implants of a porous calcium phosphate ceramic; hydroxyapatite ceramic (HAC)	A. Boyde [44]

Comments on the Models

Segmental defect models of long bone model requires osteotomy to make bone defects and needs to fix the defect ends with fixator, which makes this type of model complicated. However, in real clinical practice, fractures and bone defects usually occur on the weight-bearing bones of the extremities and internal and external fixators are frequently used in treatment. Thus, the segmental defect models are close to clinical scenarios. Besides, if the design purpose of a novel bone substitute material is to repair a long bone defect of the limbs, the segmental defect model of weight-bearing bone is more suitable. In addition, real bone fractures are often accompanied by peripheral soft tissue injury and inadequate blood supply. The middle and lower segments of the tibia are in contact with subcutaneous tissue without muscle in between, rendering the tibia defect model similar to the clinical factures.

Segmental Defect Models of Non-weight Bearing Long Bone

The non-weight-bearing bones include ulnar, radius, and the fibula. When these bones are truncated, the stability of the broken ends may not be destroyed and the defect ends usually need no fixation, which obviously simplifies the preparation process of the model. To prevent the displacement of the testing material, cerclage wires can be used to prevent dislocation during modeling [46, 47, 49].

CSD in Segmental Defect Models of Non-weight Bearing Long Bone

For mice, the shaft of the radius is most commonly used and the lengths of defects are usually 1.5 and 2.5 mm [50, 51].

For rats, 5-mm osteotomy is usually created on the bilateral radial shaft [45, 52] (Fig. 3a). Although the segmental fibular defect model has two different defect sizes (2 mm and 4 mm) [53], 4 mm is generally considered to be the CSD for fibula [1, 54]. The segmental fibular defect model can also be performed in bilateral fibular bone [54] which can reduce the required number of animals. Besides, two different materials can be compared on one individual rat, which could reduce the experimental error and make the results more consistent.

In rabbit model radius is the most commonly used bone to generate a CSD. It is generally believed that the CSD value in long bone should be at least two times the diameter of the diaphysis [46, 47, 49] (Fig. 3b, c). The radius diameter of adult New Zealand white rabbit is approximately 5–6 mm. Therefore, some scholars have determined 10 mm-defect as the CSD [16, 55–58], although 15 mm-defect has also been used [59, 60]. Moreover, the osteotomy site of the defect is suggested to be selected at 2.5 cm above the radio-carpal joint. Besides the radius, the rabbit ulnar shaft can also be used. Two sizes, 15 mm [61] and 20 mm [62], are commonly adopted as the CSD values of the ulnar. Only a few scholars adopted nonstandardized

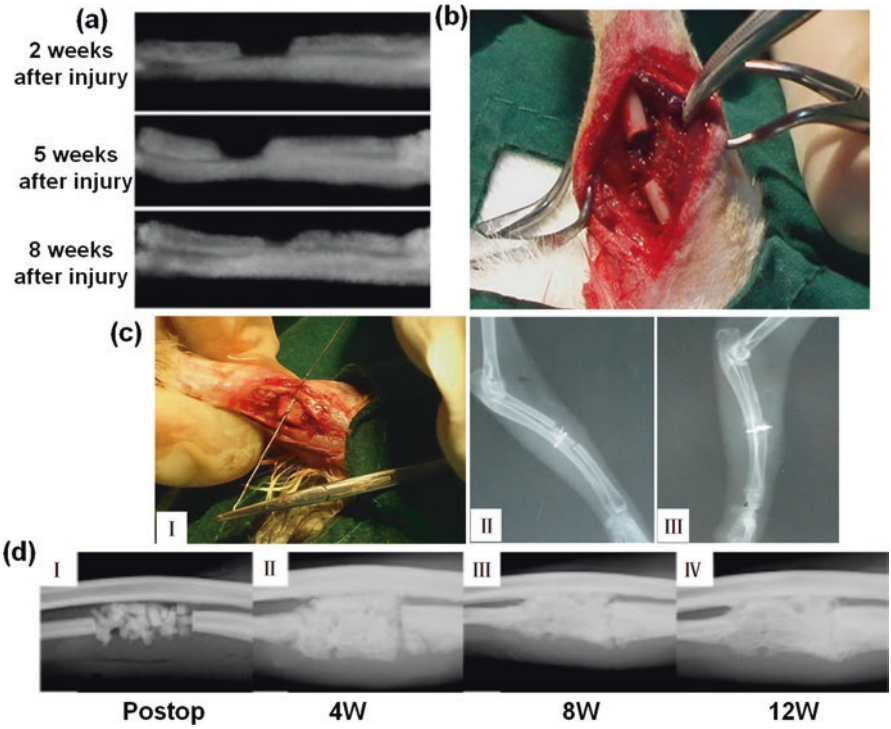

Fig. 3 Non-weight-bearing long bone segmental defect models: (**a**) Postoperative radiographs of chitosan (CS)-gelatin (Gel) scaffolds in rat radial bone defect (5 mm) at 2, 5, and 8 weeks [45]. (**b**) Radius of rabbit exposed by dissection of surrounding muscles and an osteoperiosteal segmental defect was created on the middle portion of each radius at least twice that of the diameter of the diaphysis [46]. (**c**) (I) Xenogenic growth plate grafting in radius defect of rabbit; (II–III) Radiographs of forelimb on 14th day post opertation (II-autograft, III-growth plate xenograft) [47]. (**d**) Radiographs of the postoperative changes in canine segmental ulnar defects filled with BMP and cells [48]

ulnar stem defects. For example, evaluate recombinant human bone morphogenetic protein-2 in promoting bone healing, Bouxsein et al. built a blade-width (0.5–1 mm) defect in the ulna [63].

Ulna defects are often made in dog models. The ulna is exposed through craniolateral approach [64], and the osteotomy site is located at the proximal 4 cm of the ulnar styloid process [65]. The length of the osteotomy has various sizes in literature: 20 mm [65], 22.5 mm [64], and 25 mm [48, 66, 67] (Fig. 3d). The radius of the dog can also be used to build segmental bone defects with a size of 10 mm [68].

Comments on the Models

Compared with the weight-bearing long bone defect models, the non-weight bearing long bone segmental defect models are relatively simple to create. However, the forearm defect model cannot avoid the interactions between radius and ulna, and

the pathological and biomechanical changes in one could be compensated by another. Other shortcomings of these models include the great variations in the bone diameter and resultant sizes of defects created (Table 3).

Metaphyseal Defect Model

When preparing a metaphyseal defect model, a small drill is used to make a lateral cylindrical defect which is vertical to the axis of the femoral shaft [71–74], and then the bone substitute materials with proper diameters are implanted into the cylindrical defect.

Femur or tibia is commonly selected for this model due to their large sizes and good accessibility to their condyles. The metaphyseal bone is located subcutaneously and usually no extra fixation is needed after defect creation, which makes the model relatively simple to create with a high success rate [75].

CSD in Metaphyseal Defect Models

In mice metaphyseal defect model, defects with 1 mm in diameter were usually created at the proximal tibia [76] and distal femur [77, 78]. However, these small defects are difficult to evaluate bone substitutes. These defects are mainly used to test drug or investigate the mechanism of fracture healing.

For rats, bone defects with 3.5 mm in diameter at the proximal tibial diaphysis are often used for evaluating biomaterials [79]. Bone defects with different sizes, 5 mm in diameter and 5 mm in depth [80], 6 mm in diameter and 10 mm in depth [69, 73] (Fig. 4a), and 6.1 mm in diameter [70] (Fig. 4b) were fabricated on the metaphysis of rabbit femur. The size of defect in canine femoral condyles could reach 20 mm in depth and 8 mm in diameter [81] or 20 mm in depth and 10 mm in diameter [82].

Comment on the Models

The metaphyseal defect model only simulates a bone defect environment, not a long bone fracture or defect in clinical scenarios. Only a few categories of materials are suitable for evaluating by this type of models, including bone filler or substitutes for localized bone defects, granular or colloidal materials without structural support capabilities, and bone cement, etc. Besides simple modeling without the requirement for fixation, another advantage of the condyle defect model is that it can avoid the displacement of testing material (Table 4).

Table 3 Non-weight bearing long bone segmental defect models for biomaterial evalutions and relevant references

Animal			Bone defect					
Species	Strain and age	Gender and weight	Position	Number	Size	Fixation	Experimental biomaterials	Reference
Mice	C3H/hen mice (8–10 weeks old)	Female	Radial diaphysis	One	1.5 mm long	No	Electroporated with either BMP-9 plasmid, Luciferase plasmid or injected with BMP-9 plasmid but not electroporated	K.B. Nadav [50]
	C3H/hen mice (8–10 weeks old)	Female	Radial diaphysis	One	2.5 mm long	No	One million Tet-off BMP2 MSCs were suspended in 15 mL fibrin gel that was supplemented with PFTBA or not	K.B. Nadav [51]
Rat	Wistar rats	Weighing 250 ± 25 g	Radial diaphysis	Bilateral	5 mm long	No	Gelatin, chitosan, and their combination as tissue-engineered scaffolds	A. Oryan [45]
	SD rat (10-week-old)	Male	Radial diaphysis	Bilateral	5 mm long	No	Vitamin D-binding protein (DBP) (gelatin sponge)	J. Sun [52]
	Homozygous Athymic RNU Nude rat (adult)	– (200–300 g)	Fibula diaphysis	One	2–4 mm long	No	Adenovirus-transduced cells expressing bone morphogenetic protein 2	W. Zawaunyka [53]
	Rat	– (200–250 g and 260–290 g)	Fibula diaphysis	Bilateral	4 mm long	No	7-mm-long tubular specimen of demineralized bone matrix (DBM)	D. Chakkalakal [54]
Rabbit	New Zealand Albino rabbits (12 months old)	Male (3.0 ± 0.5 kg)	On middle portion of each radius	Bilateral	At least twice as long as the diameter of diaphysis	Cercelage wire	Fresh cortical autograft and allograft	Z. Shafiei [46]
	New Zealand Albino rabbits (12 months old)	Male (3.0 ± 0.5 kg)	On middle portion of each radius	Bilateral	At least twice as long as the diameter of diaphysis	Cercelage wire using stainless wire No. 01	Autograft and new xenograft (bovine fetal growth plate)	S.N. Dehghani [47]

	NZW rabbits (12 months old)	Male (3.0 ± 0.5 kg)	On middle portion of each radius	Bilateral	At least twice as long as the diameter of diaphysis	Cercelage wire	Autograft and new xenogenic bovine demineralized bone matrix (DBM)	A.S. Bigham [49]
	NZW rabbits (12 months old)	Both sexes (2.0 ± 0.5 kg)	Radial diaphysis	Bilateral	10 mm elongation	No	Combination of human platelet-rich plasma and coral	A.M. Parizi [16]
	NZW rabbits (12 months old)	Both sexes	Radial diaphysis	Unilateral	10 mm long (CSD)	No	Human platelet-rich plasma in combination with hydroxyapatite and coral on osteogenesis	S.S. Zahra [55]
	NZW rabbits (12 months old)	Both sexes (2.00 ± 0.50 k)	In mid portion of each radius	Bilateral	10 mm long (CSD)	No	Hydroxyapatite-human platelet-rich plasma (HPRP)	A. Oryan [56]
	NZW rabbits (12 months old)	Both sexes (2.0 ± 0.5 kg)	Radial diaphysis	Unilateral	10 mm long (CSD)	No	Hydroxyapatite with demineralized calf fetal growth plate (DCFGP)	B. Amin 2015 [57]
	NZW rabbits	Male (about 3.5 kg)	Radial diaphysis	Unilateral	10 mm long	No	Barrier membranes combination with recombinant human bone morphogenetic protein 2 (rhbmp-2)	G. Zellin 1997 [58]
	New Zealand rabbit	– (6 kg)	Radius diaphysis	One	15 mm long (CSD)	No	Rhbmp-2 combined either with chitosan hydrogel (rhbmp-2/CH) and chitosan hydrogel containing β-tricalcium phosphate (β-TCP) (rhbmp-2/CH/TCP)	L. Luca [59]
	NZW rabbits (3-month-old)	Male (2.0–2.5 kg)	In middle of radial shafts	One	1.5 cm long	No	Complexes of zein scaffolds and rabbit MSCs	J. Tu [60]

(continued)

Table 3 (continued)

Animal			Bone defect					
Species	Strain and age	Gender and weight	Position	Number	Size	Fixation	Experimental bio materials	Reference
	Japanese white rabbit (16–20 week old)	Male	Ulna diaphysis	Unilateral	1.5 cm long	No	Recombinant human bone morphogenetic protein (rhBMP)-2 and a novel carrier, PLGA-coated gelatin sponge (PGS)	S. Kokubo 2003 [61]
	NZW rabbits (6-month-old)	Male (3.5–4.0 kg)	Ulna (3.0 cm from ulnocarpal joint)	Bilateral	2.0 cm long	No	Implanted with a pastelike polylactic glycolic acid blood clot combination that was mixed with five different concentrations of rh-BMP2	M. Bostrom [62]
	NZW rabbits (8–9 months)	Male	Ulna (45–50 mm distal to olecranon process)	Bilateral	Blade-width defect (0.5–1 mm)	No	An absorbable collagen sponge containing rh-BMP2	M.L. Bouxsein 2001 [63]
Canine	Female beagle dogs (1 year old)	Female (9.4–11.0 kg)	Shaft of ulna	Unilateral	2.5 cm long (CSD)	No	Escherichia coli-derived recombinant human bone morphogenetic protein-2 combined with bone marrow-derived mesenchymal stromal cells	T. Itoi [48]
	Beagle dogs (1.5–0.27 years)	(13.7–2.1 kg)	Shaft of ulna	Bilateral	22.5 mm long (CSD)	No	Bone morphogenetic protein-2 and vascular endothelial growth factor	R. E. Geuze [64]
	Labrador retrievers (32 ± 5 months)	Both gender (31 ± 1 kg)	4 cm proximal of ulnar styloid process	Bilateral	20 mm long (CSD)	No	Local continuous growth hormone administration	L. Theyse [65]

	Mixed-breed hounds	– (22.56 ± 2.22 kg)	Mid-diaphyseal of ulnar	Bilateral	2.5 cm long (CSD)	No	Recombinant human bone morphogenetic protein-2 (rhbmp-2)/absorbable collagen sponge (ACS) with cancellous allograft bone or biphasic calcium phosphate ceramic granules	C.B. Jones [66]
	Male mongrel dogs	Male (35–45 kg)	Mid-ulna	Bilateral	2.5 cm long (about 2–2.5 times midshaft) (CSD)	No	Recombinant human bone morphogenetic protein-7 (recombinant human osteogenic Protein-1, rhop-11)	S. Cook [67]
	Adult mongrel dogs (3–4 years old)	Male (25.2 ± 3.5 kg)	Mid-diaphysis of radius	One	10 mm transverse bone defect	No	Greater omentum as a scaffold incorporation of ASCs (adipose-derived adult stem cells)	B.S. Amin [68]

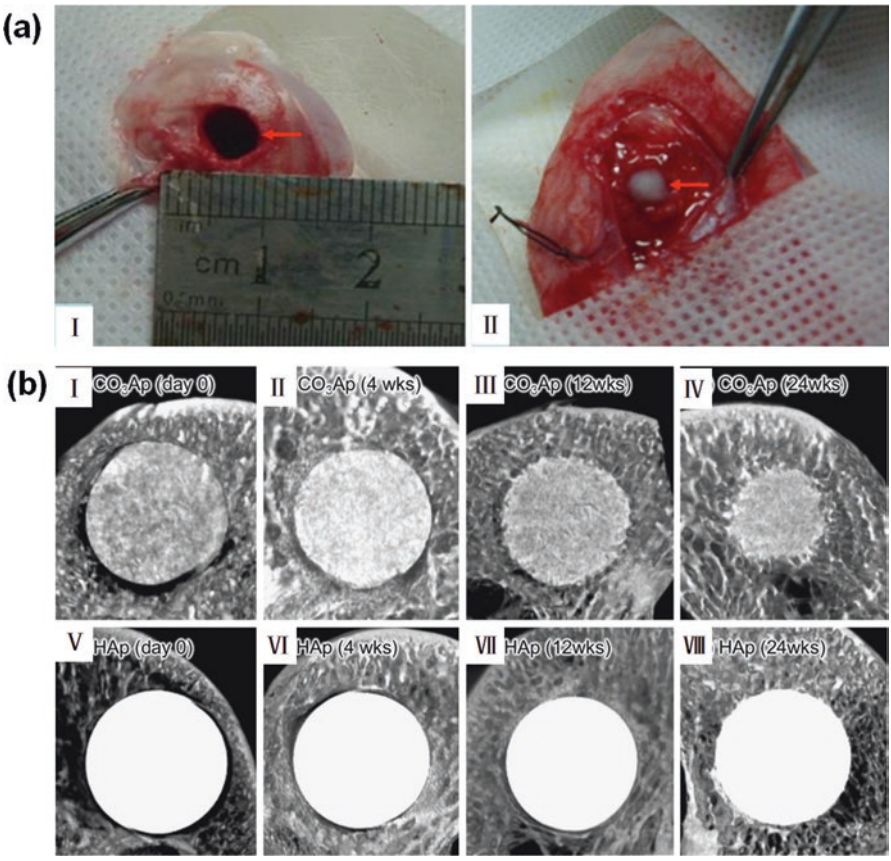

Fig. 4 Metaphyseal defect models: (**a**) Rabbit femoral condyle bone defects surgical procedure; (I) CSD (6 mm in diameter and 10 mm in length) was transversally created in the femoral condyles of rabbits; (II) the defect was filled with nHA/CS composite scaffolds [69]. (**b**) Micro-CT sagittal images of the rabbits' distal femurs from a top view of the CO_3Ap blocks (I–IV) and HAp blocks (V–VII) immediately after implantation (day 0) (I, V) and at 4 (II, VI), 12 (III, VII), and 24 (IV, VII) weeks after implantation in rabbits' distal femurs [70]

Vertebral Body Defect Models

In some studies, the injectable biomaterials were evaluated on long bone defect models [79]. However, the different parts of the bone have varied mechanical environment, which may lead to varied material degradation behavior and bone tissue response in vivo [83, 84]. To simulate the actual environment, materials specifically for vertebral repair or augmentation are strongly recommended to be evaluated by vertebral defect models (refer to [85] for illustrative images).

Table 4 Metaphyseal defect models for biomaterial evaluation and relevant references

Animal			Bone defect					
Species	Strain and age	Gender and weight	Position	Number	Size	Fixation	Experimental biomaterials	Reference
Mice	Osm and Osmr_/_ mice, backcrossed onto C57BL/6 (7–8 weeks old)	–	Proximal tibia	One	A hole with 1.0 mm in diameter	No	Mice were treated daily by intraperitoneal injection of 10 mL/g clodronate or control phosphate-buffered saline (PBS) liposomes	E. Wehrle [76]
	C57BL/six male mice	–	In the femur mid-diaphysis and the distal epimetaphyseal region	Two	0.9 mm in diameter for femur mid-diaphysis Holes with 0.9 mm in diameter, 1 mm deep for distal epimetaphyseal region	No	–	L. Monfoulet [77]
	C57BL/6N mice (7 weeks of age)	Male	At the anterior portion of the diaphysis of bilateral femurs	Two	1 mm in diameter	No	Bisphosphonate (YM529), a nitrogen-containing bisphosphonate	M. Nagashima [78]
Rat	Wistar rats	Male (body weight 350–450 g)	Proximal tibial diaphysis	One	3.5 mm in diameter	No	A full synthetic injectable bone substitute (SIBS) (like microparticles)	W. Xu [79]
Rabbit	New Zealand rabbits	2.0–2.5 kg body weight	Distal femur	One	6 mm in diameter and 10 mm in depth (CSD)	No	Injectable nanohydroxyapatite/chitosan composites scaffolds	X. Zhang [69]
	Japanese white male rabbits (19–20 weeks old)	3335 ± 322 g body weight	Distal femur	One	6.1 mm in diameter	No	Carbonate apatite blocks fabricated from dicalcium phosphate dihydrate blocks	M. Kanazawa [70]

(continued)

Table 4 (continued)

Animal			Bone defect					
Species	Strain and age	Gender and weight	Position	Number	Size	Fixation	Experimental biomaterials	Reference
	NZW rabbits (6-month-old)	Male	Distal femur	Bilateral	6 mm in diameter and 10 mm in depth (CSD)	No	β-TCP collagen composite bone substitute	H. Zheng [73]
	NZW rabbits (6-month-old)	–	Distal femur	Bilateral	5 mm in diameter and 4–5 mm in depth	No	Pthrp (107–111) (osteostatin) loaded onto silica-based ordered mesoporous SBA15 materials	C.G. Trejo [80]
Canine	Adult mongrel dogs (German shepherd type)	25–30 kg body weight	Distal epiphysis of the femur	Bilateral	8 mm in diameter and 20 mm in length	No	Skeletal fragments of different coral genera	G. Guillemin [81]
	Beagle dogs (aged 1–2 years)	Male (10–12 kg)	Femoral condyles	Bilateral	10 mm diameter (from medial to lateral)	No	Tetrapod-shaped granular artificial bone (Tetrabone®) or β-tricalcium phosphate granules (β-TCP)	S. Choi [82]

Small Animal Vertebral Body Defect Models

In small animals, rats are often used to fabricate vertebral body defect models. The CSD of rat vertebra was explored by Liang et al. [85]. Two different sizes of defect, 2 mm × 3 mm × 1.5 mm and 2 mm × 3 mm × 3 mm, were made in anterior part of L4, L5, and L6 vertebra, and the former bone defect was found to be the CSD. Besides, the bone defect model can also be constructed in the caudal vertebra of rats. For example, a cylindrical defect (1.8 mm in diameter and 2 mm in depth) in the center of the third caudal vertebra was created through a left posterolateral approach [86]. The advantages of caudal vertebra model include simple anatomy approach and free of the risk to important organs and vessels. Meanwhile, there is even simpler method of modeling, such as PMMA directly injected into the L1–L6 vertebral body of New Zealand rabbits [87]. However, the clinical significance of such modeling methods for biomaterial evalution is questionable.

Large Animal Vertebral Body Defect Models

Sheep vertebral body defect model is most frequently used. The similarity of body weight and bone size of sheep to those of humans allows testing biomaterials designed for clinical study. The L2-L5 vertebrae are usually used to create the model. Usually, a cylindrical hole with a certain diameter and depth is drilled in the center of vertebral body to simulate the space created by balloon in kyphoplasty (KP) and then the defect is filled with injectable biomaterials. The diameters of the hole include 4 mm [88], 6 mm [88, 89], 8 mm [90, 91], and 10 mm [92], while the depths of the hole are 9 mm [88], 10 mm [89], 15 mm [90–92], and even 20 mm [93].

In addition to these common cylindrical defects, the rectangular defect with 8 mm high, 10 mm deep, and 20 mm long, was used to test injectable calcium phosphate cement [94]. Verron et al. [94] built an osteoporosis vertebral bone defect model, which was in line with the fact that most of the patients receiving the treatment of bone filling material suffer from osteoporosis. However, the establishment of this osteoporotic model needs a long modeling time (4–6 months) and high costs.

Canines are less used in vertebral defect model than sheep. In the modeling process, the lateral side of the lumbar spine is shown through the dorsal to the transverse process. The central vertebral defect with the size of 18 mm × 5 mm × 22 mm was produced, and the researcher injected the biomaterial into the defect for testing [95].

The bone defect in swine vertebral body can be created by percutaneous puncture under fluoroscopic guidance [96]. The lumbar vertebrae of mini-swine were also used for preparing defect model (15 mm in depth and 4 mm in diameter) [97]. Compared with other species, swine models are noisier and more aggressive, and their daily management is more difficult [98] (Table 5).

Table 5 Vertebral body defect models for biomaterials evalutions and relevant references

Animal			Bone defect					
Species	Strain and age	Gender and weight	Position	Number	Size	Fixation	Experimental biomaterials	Reference
Rat	Fischer rats (6-months-old)	Male	In anterior part of VB (L4, L5, and L6)	Three	A large defect (2 mm deep × 3 mm wide × 3 mm long, CSD) and A small defect (2 mm deep × 3 mm wide × 1.5 mm long)	No	Sintered poly(lactic-*co*-glycolic acid) (PLGA) microsphere scaffolds loaded with Matrigel with or without recombinant human bone morphogenetic protein 2 (rhbmp2; 2.0 μg rhbmp2/10 μL Matrigel/scaffold)	H. Liang [85]
	Mature athymic nude rats	–	In center of third caudal vertebral body (Ca3)	One	1.8 mm in diameter and 2 mm-deep cylindrical defect	No	The ASCs were first labeled with reporter genes and then nucleofected with an rhbmp6-encoding plasmid. The ASC-BMP6 cells were suspended in fibrin gel (FG)	D. Sheyn [86]
	Wistar rats	Male (300–350 g)	L2 vertebra	One	2 × 5 × 1.5 mm^3	No	A composite bioartificial graft based on a hydroxyapatite bone scaffold (CEM-OSTETIC_) combined with human mesenchymal stem cells (MSCs)	V. Vaněček [99]
Rabbit	New Zealand rabbits (0.7–1.1 years, mean 1.0 year)	Female (weight: 2.3–2.8 kg)	L1–L6 vertebrae	Six	1 mL syringe injected 0.5–0.6 m PMMA into vertebrae	No	PMMA	R. Quan [87]
Canine	Skeletally mature large hounds	– (30–41 kg)	In the vertebral bodies of L1 and L3 just dorsal to the transverse process	Two	Central vertebral defect nominally measuring 18×5×22 mm^3	No	Cap or PMMA cement	T.M. Turner [95]
	Sheep (2.5 years old ± 0.5)	40–50 kg	L2 to L5 vertebrae	Four	6 mm in diameter and 9 mm in depth	No	Material consists of calcium sulfate and β-tricalcium phosphate (β-TCP)	H.L. Yang [88]

Sheep	Adult female sheep (an average age of 2.5 ± 0.5 years)	40–50 kg	Center of the L2-L5 lumbar vertebra	Four	6 mm in diameter, 10 mm in depth	No	Calcium phosphate (cap), calcium sulfate (cas), and polymethylmethacrylate (PMMA)	X. Zhu [89]
	Female Rambouillet X Columbia Sheep (about 3.5 years old)	Mean 79.0 kg	L3, L4, and L5 vertebral bodies	Three	8 mm in diameter and depth of 15 mm	No	Calcium sodium phosphosilicate putty with or without autograft and NovaBone 45S5 Bioglass Particulate (Novabone, LLSSSSSC, Jacksonville, FL)	H. Kobayashi [90]
	Skeletally mature female Rambouillet X Columbian ewes	60–80 kg	In lateral cortex of L3 and L5	Two	8 mm in diameter and depth of 1 cm drilled hole	No	Calcium phosphate bone cement (Bone-Source1 (CPC); Stryker Orthopaedics, Mahwah, New Jersey) plus carboxymethyl cellulose (CMC)	H. Kobayashi [91]
	Male sheep (2.5 years old)	110–150 lb	L3, L4 and L5	Three	10 mm in diameter and 15 mm deep	No	Bioactive glass based composite putty (NovaBone Putty) compared to NovaBone (a bioactive glass particulate)	Z. Wang [92]
	Sheep (4-year-old sheep)	Mean 75 kg	Central portion of L2 and L4	Two	2.0 cm in diameter	No	Hyaluronic acid (HA) with hydroxyapatite-coated β-tricalcium phosphate (β-TCP), or material of rhnell-1 protein lyophilized onto β-TCP mixed with HA	A.W. James [93]
	Ovariectomized adult female sheep	–	L3 and L4 vertebral bodies	Two	8 mm high × 10 mm deep × 20 mm long,	No	Injectable alendronate-doped calcium phosphate cement	E. Verron [94]
Swine	Porcine species crossing Pietrain breed	Female	L3 vertebral body	One	An anterior defect of 1 cm^3	No	Tricalcium phosphate, tricalcium phosphate with bone morphogenetic protein (rhBMP-7) and autologous bone marrow aspirate with rhbmp-7	E. Manrique [96]
	Miniswines	–	Lumbar vertebra	One	15-mm in depth and 4-mm in diameter cylindrical bone defect	No	Mesenchymal stem cells overexpressing the BMP6 gene (MSC-BMP6)	G. Pelled [97]

Other Bone Defect Models

Femoral Wedge Bone Defect Model

Volker et al. produced femoral wedge bone defect model in rat to resemble clinically relevant situations of osteoporotic bone [100]. In Volker's research, a 5-mm wedge-shaped osteotomy as critical size defect was conducted at the distal metaphyseal area of rat femur and fixed using a T-shaped plate.

Multiple-Defect Model in Canine Femur and Tibia

Bone defects could be established at various sites on canine bones. The middle section of the femur can produce two bone defects with 4-mm in diameter for testing biomaterials [101]. The canine femoral multiple defect (CFMD) is in the lateral cortex of the upper segment of the femur. During modeling, a specific device is fixed to the lateral cortex of the proximal femur by two screws: one upper and one lower. The four consecutive fabricated bone defects are cylindrical with 10 mm in diameter and 15 mm in length [102–104]. In addition, each bone defect is at least 1.5 cm [102] or 1.2 cm [105] apart from the normal bone and bone marrow. This model is suitable for evaluating different materials in the same animal at the same time. Thus, accurate data comparison could be reached, and the number of animals could also be reduced. It is also an effective comparison tool for the evalution of cell delivery [103] and growth factor delivery [102, 105].

The canine tibia could also be used to prepare tibil a multiple-defect model (CTMD) [106]. In a previous study, the tibia was exposed via a medial approach, and then an electrical motor was used to create consecutive cylindrical bone defects with 4 mm in diameter, where different materials could be implanted at the same time [106].

Nonunion Models

The short stumpy limbs of swine might restrict the creation of standard CSD models. Thus, some special models, such as nonunion model, have emerged. Schubert et al. [107] created a critical bone defect with a size 1.5 times that of the diameter of the femoral shaft in miniature swine (aged not older than 6 months and weighing $\leq$50 kg) and used two 4.5-mm locking compression plates for stabilization. Canines can also be used to produce nonunion model. Saifzadeh et al. produced a 2-mm transverse defect in the right medial radial diaphysis [108], where the defect ends were not fixed to create a nonunion model for testing autogenous greater omentum (Table 6).

Table 6 Other bone defect models

Category	Animal information		Bone defect				Experimental biomaterials	Reference
	Strain and age	Gender and weight	Position	Number	Size	Fixation		
Rat femoral wedge bone defect model	Ovariectomized SD rat (10-week-old)	Female	Distal metaphyseal area of femur	One	3 or 5 mm wedge-shaped osteotomy	T-shaped mini-plate	–	V. Alt [100]
Canine femur diaphyseal local defect model	–	–	Mid-diaphyseal of femur	Two	4 mm in diameter	No	Calcium phosphate cement	H. Yuan [101]
Canine femoral multi-defect model (CFMD)	Coonhounds (mean 1.9 years, 1–3 years)	Female (31.6 ± 2.2 kg)	In metaphysis and proximal diaphysis of the femur	Four (outer edge of each defect was 1.5 cm from adjacent defect)	10 mm diameter ∗ 15 mm long unicortical cylindrical defects	No	A scaffold comprising rhbmp-2/ACS in which the sponge wraps around tricalcium phosphate hydroxyapatite granules (rhBMP-2/ACS/TCP-HA)	V. Luangphakdy [102]
	Coonhounds (age 2–4)	Female (32.1 ± 1.8 kg)		Four	10 mm in diameter and 15 mm in length cylindrical defects	No	Mineralized cancellous allograft (MCA) used as an osteoconductive carrier scaffold for loading of HA-positive cells	T. Caralla [103]
	Coonhounds (age 2.5 years–01 months) (range 1–5 years)	Female and male (34.3 ± 4.2 kg)		Four	10-mm-diameter and 15-mm-long defects	No	Poly(L-lactide-*co*-glycolide) (PLGA), poly(L-lactide-*co*-e-caprolactone) (PLCL), tyrosine-derived polycarbonate (tyrpc), and poly(propylene fumarate) (PPF) Highly porous three-dimensional (3D) scaffolds	V. Luangphakdy [104]

Table 6 (continued)

Category	Animal information		Bone defect				Experimental biomaterials	Reference
	Strain and age	Gender and weight	Position	Number	Size	Fixation		
	Adult mongrel dogs	Male (30.0–35.8 kg)		Four (outer edge of each defect was 1.2 cm from adjacent defect)	1.0-cm diameter and 1.0-cm deep cylindrical defects	No	The OP-1 (3.5 mgrhop-1 in 1 g β sheep collagen I matrix) was implanted in each site combined with either clotted blood or aspirated bone marrow (BM)	H. Takigami [105]
Canine tibia multi-defect model (CTMD)	Mongrel dogs (2–3 years old)	Male (26.2 ± 2.5 kg)	From stifle to metatarsal region in tibia	Seven	4 mm in diameter of circular bone defect	No	Xenogenic bovine fetal demineralized bone matrix (DBM), commercial DBM, omentum, omentum-calf fetal DBM, cortical autograft, and xenogenic cartilage powder	B.S. Amin [106]
Nonunion models	MGH-miniature swine (<6 months)	<50 kg	In the mid-diaphysis of one femur	One	A critical bone defect of 1.5 times the diameter of the femoral shaft	Two 4.5-mm locking compression plates positioned on anterior and lateral sides	3D osteogenic differentiated AMSC (osteoblastic differentiated adipose mesenchymal stem cells) autograft	T. Schubert [107]
	Adult mongrel dogs	Male	Right medial radial diaphysis	One	2-mm transverse bone defect	No	Autogenous greater omentum as a free nonvascularized graft	S. Saifzadeh [108]

Selection of Bone Defect Model

A suitable bone defect model for biomaterials and tissue engineering study is critical. The selection of bone defect model involves the considerations of characteristics of animal models, research purposes, and biological characteristics and design specifications of bone substitute materials.

Age and Sex of Animal

The bone repair ability is very high in young animals. For rats, the speed of bone repair in immature bones was more than that of the mature ones [109, 110]. For example, the healing time of femoral fractures is only 4 weeks for 6-week-old rats, whereas the healing time is 26 weeks for 52 week-old rats [111]. The similar results have been found in rabbit models [112], which might be related to the varied secretion of bone morphogenetic protein (BMP) [113]. The ability of fast bone repair could affect the test results of bone substitute material. Therefore, adult rats were usually selected in the establishment of bone defect models [1, 109, 114, 115]. Similarly, rabbit bone growth stops within 19–32 weeks [116] and therefore 6–9 month-old male rabbits are usually selected for study [72, 73].

Estrogen cycle also has a significant effect on bone repair and turnover. In ovariectomized rats, particularly in elderly rats, the delayed union of the femoral fractures and reduction of bone mineral density (BMD) would occur [117]. Therefore, the ovariectomized rats were often used to establish osteoporotic fracture models. Studies on non-osteoporotic bones should select male animals to avoid this interference. But it is worthy mentioning that male animals usually have a strong sense of territory and the use of individual cages may be required to prevent fights, injuries, or even deaths among male animals. Thus, the age and sex of the animal should be well controlled for study and reported in details.

Comparison between Different Animal Species

In bone tissue engineering and osteoinductive biomaterial researches, the animal species used for model is also critical for reliable and consistent results. The animals of each species have their own unique skeletal characteristics including bone morphology, bone microstructure, bone turnover, and bone remodeling. The ideal animal for bone defect model should have bone characteristics highly similar to that of human, in order to guarantee that the results of animal experiments could be safely extrapolated to humans. However, the availability, costs, and ethical consideration will also be involved in the selection of animal species. A general summary of various commonly used species is provided below.

Rodents

There is a great discrepancy between the bone microstructures of rodents and human. Different from the osteon structure in adult humans, the long bone cortex of rats consisted mainly of primary and cancellous bone, which lacks a Haversian canal system [118].

Intramembrane and endochondral ossifications are two typical bone formation mechanisms during fracture healing [119]. In the fracture healing of rodents, endochondral ossification is more predominant although both kinds of fracture healing mechanisms are present [120, 121]. The bone healing capability of rodents is greater than that of human [1]. Unlike human bone that ceases to grow after sexual maturity, the bones of the sexually mature rodent would continue to grow for extended time [122].

Mice are inexpensive and widely available, easy to manage, and have pure strain and strong infection-resistance. The mouse genome is also thoroughly researched, and it means that bone substitute material can be studied at the molecular level. When the inbred line mice are used in the model, the differences between individuals are small, which makes the results more reliable. Furthermore, nude mice are well-developed animal model that has no immunological rejection for bone tissue engineering substitutes that incorporated with human cells. However, the mouse skeleton is too small to establish a large defect model. Moreover, for some bone implants, shrinking to the appropriate size of the defect to evaluated the clinical outcome is difficult [123]. In addition, compared with mouse model, the rat model has better practical value in biomechanical tests.

Rabbit

Both the macro- and microstructure of rabbit's bones are distinctly different from those of human [124]. Unlike the mature human bones with secondary hierarchical structure, rabbit skeletal bone has a primary vascular longitudinal tissue structure. It forms a vascular access to the Haversian canal that is wrapped around the medullary cavity and distributed on the periosteal surface [125]. The bones between these lamellar structures are composed of dense Haversian bone [125]. However, the bone structure of rabbit is still more representative for human than that of mouse [126].

Compared with primates and rodents, rabbits have faster bone remodeling, particularly in Haversian remodeling of cortical bones [127–129]. Thus, it is not advised to extrapolate from the rabbit's findings to possible human clinical responses [130].

Rabbits are easy to manage, and the cost is less than larger animals. Compared with rodents, the biggest advantage of rabbit is the large size of bones that benefits for bone defect creation. Also, the ear margin vein of rabbit is convenient for obtaining blood samples, which is beneficial for blood analysis.

Canine

Canine bone components are highly similar to those of humans, including hydroxyproline, extractable proteins, IGF-1 content [131], as well as water fraction, organic fraction, volatile inorganic fraction, and ash fraction [132]. Microscopically, canine bone has secondary osteonal structures, known as plexiform bone or laminar bone in the adjacent endosteum and periosteum [124]. The plexiform bone is found in the rapid growth of children, or in rapidly growing large animals [133]. Therefore, canine bone is considered as one of the best representatives of human bone structure [131]. Thus, dogs are suitable for animal models in biomaterials research and bone tissue engineering. However, canine bone defect models have not been widely used due to the high costs and difficult breeding as well as ethical limitations in some countries.

When using canine as animal model, it should be noted that bone remodeling process of dogs is quite different from that in humans. The mean bone turnover rate of young adult female beagles is much higher than that of humans [134, 135], which could partially explain the high fusion rates in canine lumbar fusion models and the low nonunion rates [98]. The rate of bone remodeling in different bones varies significantly for dogs. Considering adult male beagles, the bone turnover rate is close to 200% and 12% annually in the lumbar vertebra and talus, respectively. Although, the mean total turnover of trabecular bone is approximately 100% annually [134].

Goat and Sheep

Sheep and goats have the similar weight as humans, and their limbs can provide sufficient testing space for clinically sized implants [128, 136, 137]. The structure of sheep bone is remarkably different from that of human histologically. Compared with human bone that mainly consists of secondary bone structure [138], the sheep bone has mostly primary bone structure where osteons is <100 μm in diameter and contains at least two central blood vessels. Bone structure changes in sheep are related to age. Before the age of 3–4 years, the sheep's plexiform bone structure consists of a combination of woven and lamellar bone with sandwiched vascular plexuses [128]. When the sheep is 7–9 years old, Haversian remodeling occurs [128] and becomes more common as age increases [139]. Furthermore, the location of bone remodeling seemed to vary with bone types and the earliest indications of remodeling include the distal femur, radial shaft, and humerus [128]. Similar to sheep, the Haversian systems of goats are unevenly distributed in the whole skeleton, which mainly located in skull and the medial part of tibial shaft [140]. After comparing sheep with menopausal women in terms of bone mass, bone volume, and mineral deposition rate, Turner et al. concluded that old sheep were suitable as models for osteoporosis in the elderly [141].

Although the microscopic structure of sheep bone is different from humans, many studies have confirmed that bone turnover and remodeling activities in the sheep model are similar to those of humans [142], which makes the sheep as a valuable

model animal for testing bone substitutes [136, 143]. Although the amount of bone ingrowth in sheep was greater than that in humans, Willie et al. found that sheep and humans had similar patterns in terms of bone ingrowth into porous implants [144]. Lamerigts et al. found similar sequences of events occurring in humans and goats for bone grafts [145]. Furthermore, Dai et al. found that the bone healing capacity and the blood supply of goat tibia were both similar to those of humans [38].

There are some differences between goats and sheep, including microscopic structure, bone metabolism, and remodeling. However, these two models were very similar in general. Therefore, choosing goats or sheep as animal models depends on availability and other personal preferences.

Swine

Compared with sheep model, swine model are closer to humans in bone morphology, bone metabolism, bone healing, and remodeling [98, 146, 147]. The cross-sectional diameter and area of femur are very similar to those of human [148]. In mature bone, the swine have well-developed Haversian systems [149] and a layered bone structure similar to human [150]. Furthermore, its bone density and bone mineral content are almost equal to those of human bones [131], although the trabecular meshwork of swine is denser than that of humans [151]. The bone growth rate in swine is 1.2–1.5 mm daily, which is comparable to that of human beings (1.0–1.5 mm daily). The processes of bone remodeling in swine, including trabecular and intracortical basic multicellular remodeling units (BMU) based remodeling, are all similar to those in humans [150, 151]. Moreover, mineralization rate of cortical bone was the same as that in humans [152]. Thus, swines are considered suitable models for bone-related studies [147].

Nevertheless, pigs weighing over 150 kg are considered not suitable to produce animal models for biomaterials and bone tissue engineering study. Even for miniature swine, the daily management is difficult, particularly because they are noisy and aggressive. Thus, in many cases sheep and dogs are preferred over swine as large animal models [128, 153].

Small animals, such as mice, rat, and rabbits account for >70% [154, 155] of all the animal models. In general, the advantages of small animals include good affordability, convenient management, and small individual difference. However, some problems exist when using small animal model to test the potential clinical products. Considering cell-seeded scaffolds for example, the viability and osteogenic potential of cells in small scaffolds are easy to maintain to repair bone defects in small animals but it becomes difficult in large scaffolds used for large bone defect repair. Besides, small animals have strong bone healing ability and weak immune response, which is different from the actual bone repair of the human body.

For large animal models, such as sheep, dogs, and swine, its large bones would allow the evaluation of implants with the size close to those used in humans. Moreover, compared with small animals, large animal bones have

higher similarity to human bones. Although with many advantages, large animal models were not usually used due to the difficulties of accommodation, management, availability, and ethics.

Research Related Criteria

For experiments that are expected to get results in a short time, the small animal model (rodents and rabbits) is recommended due to their fast bone healing process. When long-term observation is required, large animal models are recommended, since the bone structure, bone repair mechanism, and immune response in large animals are closer to those in human body.

The study purpose of osteoinductive biomaterials and bone tissue engineering is also an important factor when choosing the model. If the experiment was to test the osteoinductive capability of the materials, skull defect models or long bone metaphyseal defect model could be used to simplify the experimental procedure.

However, more complicated models are needed for studies with specific research goals. For example, long bone segmental defect model should be utilized to test the substitute materials designed to repair long bone defects, in which fixation devices would be utilized to fix the ends of defects to simulate clinical practice. When bone substitute materials are used as bone cement for vertebroplasty (VP) and kyphoplasty (KP) surgery, the vertebral defect models are recommended.

The characteristics of materials also affect the selection of models. If the bone substitute materials were colloidal, shapeless granule, or powder, the long bone metaphyseal defect model or the multiple defect model might be a better choice, since it can avoid the dislocation and loss of biomaterials or scaffolds.

For materials containing human tissue cells, nude rodent model may be suitable models to prevent the immune system from interfering with cells. Nude rodent models are capable of ignoring the source of cells and the reaction between scaffold and the host; hence, it could be used to study the efficacy of engineered tissue products directly [156]. However, because nude rodents are immune-deficient animals and cannot reflect the normal immune functions, the data obtained from nude rodent models may need to be further confirmed by other animal models.

Bone Defect Models Simulating Clinical Scenarios

Actual Situation of Bone Defect in Clinical Settings

It should be recognized that most fractures were simple two-part fractures or minor comminuted fractures without bone defects. Bone defect is usually caused by comminuted broken ends of the fracture. In fact, serious violent injuries not only cause

fracture end comminution, but also force the fractured fragment to move, rendering it impossible to maintain the position of the broken ends.

When the bone defect exceeds the self-repairing ability, nonunion would occur without external intervention therapy. However, the bone defect size is not the only factor that affects bone healing. The real bone defect is accompanied by severe damage of blood supply at the broken ends of the fracture, which would seriously hamper the fracture healing. Therefore, the occurrence of bone defect and fracture healing are not simple processes in clinical practice. Unfortunately, most of the current bone defect models did not well imitate the actual state of clinical bone defects.

Fracture Model and Nonunion Model

There are two models that simulate the actual state of a bone fracture: closed fracture model and nonunion model. The closed fracture model is the most widely used animal model for the study of fracture healing, which is caused by exerting strength damage without incision to completely simulate the clinical practice. To make consistent fracture models, Jackson made fracture of rat femur on a force-controllable blunt guillotine device after inserting intramedullary needle into marrow cavity [157]. Bonnarens and Einhorn [158] improved the device to make the whole modeling tool portable and easy to operate. Thus, the tools and concepts of closed fracture model making have been adopted by many scholars. Marturano et al. [159] made further improvements to the fracture device, making it suitable for preparing models on the femur of mice. The tibia of mouse may also be used to make a fracture model using similar methods [160–163]. Compared with femur, the location of tibia has less muscle attachment. However, the tibia is not an ideal model for fracture-related research due to the curved long axis, complicating the biomechanical test and the insufficient soft tissue around the bone [164, 165]. Furthermore, the fibula is accidentally fractured at a rate up to 30% during the modeling process, which can change the healing rate of the tibia [166].

For creating nonunion model, closed [167–169] or open [170] fractures are created first. Subsequently, the 2-mm periosteum of the two fracture ends are cauterized and corroded, which destroy the blood supply at the fracture ends, resulting in atrophic nonunion [167–170]. These nonunion models are obviously different from the nonunion caused by severe trauma in clinical practice, which causes not only the crushing of fracture ends, but also large segmental bone defects, and destroys the blood supply around the broken ends.

Fracture-Bone Defect Models

Closed fracture models can simulate the fractures seen in clinical practice. However, the closed fracture models are suitable for fracture healing research without space for implanting biomaterial or bone tissue engineering scaffolds. More importantly,

these fracture models can self-heal without external intervention. Although current nonunion models cannot self-heal, they are not consistent with the clinical practice. Fracture defect models mimicking the clinical scenarios are still lacking.

For producing fracture-defect model, fracture is first produced. Blunt guillotine and three-point bending are classic methods of creating fractures, and the tools are simple and easy to operate. However, unlike aforementioned fracture models that have transverse fracture, fracture-defect models aim to create comminuted fracture. After creating the fracture, open operation can be used to expose the fracture ends and remove the broken pieces of bone to create a bone defect. The incision at the broken ends can be regarded as an open fracture, which is consistent with the open fractures in severe traumatic injury. Fracture-defect model can use tibia to prepare. This is because tibia has less muscle encircling, convenient positioning and is directly located in the subcutaneous tissue, which makes the removal of broken bones much easier. In clinical practice, the open comminuted fracture also occurs mostly in the tibia.

Challenges and Future Prospects

There is no standard answer for how much bone should be removed to reach the state of nonunion. In bone defect model, there is a concept of CSD and CSD values have been established in many animal models. While in fracture defect models, the factors affecting bone healing include not only the size of the defect, but also the degree of soft tissue injury at the fracture ends. Unfortunately, quantification of soft tissue damage in the process of modeling is difficult.

The present fracture creation tools are designed for small animal models. When produce similar models in large animals, redesign and development of new tools becomes necessary. However, it is not known whether the previous classical weight fall and the three-point bending principle are applicable to or effective on large animal models. In addition, small animals, such as mice and rats, used for fracture model have less individual difference and high repeatability. When fracture defect model is made using large animals, the individual difference between animals enlarges and the repeatability of the model decreases.

Summary

Compared with other animals, canine and swine are closer to humans in bone morphology, bone metabolism, fracture healing, and remodeling. However, the rat model is the most widely used bone defect model in the study of biomaterials and bone tissue engineering. It can be seen that in the actual selection of animal models, the factors that need to be considered are multifaceted. In the selection of animal species, researchers should consider the ultimate purpose of the biomaterial evalution, the material characteristics, their own facility capacity, costs and other resources.

In addition, it should be recognized that there is a significant difference between the animal bone defect models and clinical. In the future, the development of fracture defect models that are close to clinical reality may be come possible, making the evaluation results more reliable for the studies of biomaterials and bone tissue engineering.

Acknowledgements This work is supported by the National Natural Science Foundation of China (81622032, 51672184 and 81501858), Jiangsu Innovation and Entrepreneurship Program, National Basic Research Program of China (973 Program, 2014CB748600), Suzhou Science and Technology Project (SYS2019022), and the Priority Academic Program Development of Jiangsu High Education Institutions (PAPD).

References

1. Schmitz JP, Hollinger JO (1986) The critical size defect as an experimental model for craniomaxillofacial nonunions. Clin Orthop Relat Res 205:299
2. Schmitz JP, Schwartz Z, Hollinger JO, Boyan BD (1990) Characterization of rat calvarial nonunion defects. Cells Tissues Organs 138:185–192
3. Trotta DR, Gorny C Jr, Zielak JC, Gonzaga CC, Giovanini AF, Deliberador TM (2014) Bone repair of critical size defects treated with mussel powder associated or not with bovine bone graft: histologic and histomorphometric study in rat calvaria. J Craniomaxillofac Surg 42:738–743
4. Guanghui L, Xi W, Jian C, Zhaoyu J, Dongyang M, Yanpu L et al (2014) Coculture of peripheral blood CD34+ cell and mesenchymal stem cell sheets increase the formation of bone in calvarial critical-size defects in rabbits. Br J Oral Maxillofac Surg 52:134–139
5. Liu X, Zhou S, Li Y, Yan J (2012) Stromal cell derived factor-1α enhances bone formation based on in situ recruitment: a histologic and histometric study in rabbit calvaria. Biotechnol Lett 34:387–395
6. Cui L, Liu B, Liu G, Zhang W, Cen L, Sun J et al (2007) Repair of cranial bone defects with adipose derived stem cells and coral scaffold in a canine model. Biomaterials 28:5477–5486
7. Liping X, Daisuke U, Sylvain C, Collin HB, Lyndon C, Liisa K et al (2014) Fibroblast growth factor-2 isoform (low molecular weight/18 kDa) overexpression in preosteoblast cells promotes bone regeneration in critical size calvarial defects in male mice. Endocrinology 155:965–974
8. Liao YH, Chang YH, Sung LY, Li KC, Yeh CL, Yen TC et al (2014) Osteogenic differentiation of adipose-derived stem cells and calvarial defect repair using baculovirus-mediated coexpression of BMP-2 and miR-148b. Biomaterials 35:4901–4910
9. Stephan SJ, Tholpady SS, Ce GBA, Botchway EA, Nair LS, Ogle RC et al (2010) Injectable tissue-engineered bone repair of a rat calvarial defect. Laryngoscope 120:895–901
10. Jun Z, Gang S, Changsheng L, Shaoyi W, Wenjie Z, Xiaochen Z et al (2012) Enhanced healing of rat calvarial defects with sulfated chitosan-coated calcium-deficient hydroxyapatite/bone morphogenetic protein 2 scaffolds. Tissue Eng Part A 18:185–197
11. Josephine F, Zhi Y, Shihjye T, Charisse T, Nimni ME, Mark U et al (2014) Injectable gel graft for bone defect repair. Regen Med 9:41–51
12. Glowacki J, Altobelli D, Mulliken JB (1981) Fate of mineralized and demineralized osseous implants in cranial defects. Calcif Tissue Int 33:71–76
13. Sakata Y, Ueno T, Kagawa T, Kanou M, Fujii T, Yamachika E et al (2006) Osteogenic potential of cultured human periosteum-derived cells—a pilot study of human cell transplantation into a rat calvarial defect model. J Craniomaxillofac Surg 34:461–465

14. Chim H, Schantz JT (2006) Human circulating peripheral blood mononuclear cells for calvarial bone tissue engineering. Plast Reconstr Surg 117:468–478
15. Mhawi AA, Peel SA, Fok TC, Clokie CM (2007) Bone regeneration in athymic calvarial defects with Accell DBM100. J Craniofac Surg 18:497–503
16. Parizi AM, Oryan A, Shafiei-Sarvestani Z, Bigham AS (2012) Human platelet rich plasma plus Persian Gulf coral effects on experimental bone healing in rabbit model: radiological, histological, macroscopical and biomechanical evaluation. J Mater Sci Mater Med 23:473–483
17. Berner A, Woodruff MA, Lam CXF, Arafat MT, Saifzadeh S, Steck R et al (2014) Effects of scaffold architecture on cranial bone healing. Int J Oral Maxillofac Surg 43:506–513
18. Lin CY, Chang YH, Li KC, Lu CH, Sung LY, Yeh CL et al (2013) The use of ASCs engineered to express BMP2 or TGF-β3 within scaffold constructs to promote calvarial bone repair. Biomaterials 34:9401–9412
19. Nick T, Ryo J, Riddhi G, Lukasz W, Fabio L, Charles M et al (2013) Modification of xenogeneic graft materials for improved release of P-15 peptides in a calvarium defect model. J Craniofac Surg 25:70–76
20. Tanuma Y, Matsui K, Kawai T, Matsui A, Suzuki O, Kamakura S et al (2013) Comparison of bone regeneration between octacalcium phosphate/collagen composite and β-tricalcium phosphate in canine calvarial defect. Oral Surg Oral Med Oral Pathol Oral Radiol 115:9–17
21. Sato K, Urist MR (2003) Induced regeneration of calvaria by bone morphogenetic protein (BMP) in dogs. Clin Orthop Relat Res 187:301
22. Kinsella CR, Bykowski MR, Lin AY, Cray JJ, Durham EL, Smith DM et al (2011) BMP-2-mediated regeneration of large-scale cranial defects in the canine: an examination of different carriers. Plast Reconstr Surg 127:1865
23. Mulliken JB, Glowacki J (1980) Induced osteogenesis for repair and construction in the craniofacial region. Plast Reconstr Surg 65:553–560
24. Freeman E, Turnbull RS (2010) The value of osseous coagulum as a graft material. J Periodontal Res 8:229–236
25. Turnbull RS, Freeman E (2010) Use of wounds in the parietal bone of the rat for evaluating bone marrow for grafting into periodontal defects. J Periodontal Res 9:39–43
26. Livingston TL, Gordon S, Archambault M, Kadiyala S, Mcintosh K, Smith A et al (2003) Mesenchymal stem cells combined with biphasic calcium phosphate ceramics promote bone regeneration. J Mater Sci Mater Med 14:211–218
27. Komaki H, Tanaka T, Chazono M, Kikuchi T (2006) Repair of segmental bone defects in rabbit tibiae using a complex of -tricalcium phosphate, type I collagen, and fibroblast growth factor-2. Biomaterials 27:5118–5126
28. Li X, Feng Q, Liu X, Dong W, Cui F (2006) Collagen-based implants reinforced by chitin fibres in a goat shank bone defect model. Biomaterials 27:1917–1923
29. Liu G, Zhao L, Zhang W, Cui L, Liu W, Cao Y (2008) Repair of goat tibial defects with bone marrow stromal cells and β-tricalcium phosphate. J Mater Sci Mater Med 19:2367–2376
30. Sarban S, Senkoylu A, Isikan UE, Korkusuz P, Korkusuz F (2009) Can rhBMP-2 containing collagen sponges enhance bone repair in ovariectomized rats?: a preliminary study. Clin Orthop Relat Res 467:3113
31. Rena S, Jessica G, Alan E, Chu TMG, Shawn G (2011) Increasing vascularity to improve healing of a segmental defect of the rat femur. J Orthop Trauma 25:472
32. Vaida G, Micah M, Alan I, Fangjun L, Nicola P, Damian G et al (2012) Improved healing of large segmental defects in the rat femur by reverse dynamization in the presence of bone morphogenetic protein-2. J Bone Joint Surg Am 94:2063–2073
33. Corinne S, Lashan SC, Olabisi RM, Kayleigh S, Zawaunyka L, Zbigniew G et al (2013) Rapid healing of femoral defects in rats with low dose sustained BMP2 expression from PEGDA hydrogel microspheres. J Orthop Res 31:1597–1604
34. Angle SR, Sena K, Sumner DR, Virkus WW, Virdi AS (2012) Healing of rat femoral segmental defect with bone morphogenetic protein-2: a dose response study. J Musculoskelet Neuronal Interact 12:28–37

35. Duan Z, Zheng Q, Guo X, Li C, Wu B, Wu W (2008) Repair of rabbit femoral defects with a novel BMP2-derived oligopeptide P24. J Huazhong Univ Sci Technol Med Sci 28:426–430
36. Amaia C, Reichert JC, Epari DR, Siamak S, Arne B, Hanna S et al (2013) Polycaprolactone scaffold and reduced rhBMP-7 dose for the regeneration of critical-sized defects in sheep tibiae. Biomaterials 34:9960–9968
37. Berner A, Reichert JC, Woodruff MA, Saifzadeh S, Morris AJ, Epari DR et al (2013) Autologous vs. allogenic mesenchymal progenitor cells for the reconstruction of critical sized segmental tibial bone defects in aged sheep. Acta Biomater 9:7874–7884
38. Dai KR, Xu XL, Tang TT, Zhu ZA, Yu CF, Lou JR et al (2005) Repairing of goat tibial bone defects with BMP-2 gene–modified tissue-engineered bone. Calcif Tissue Int 77:55–61
39. Zhu L, Liu W, Cui L, Cao Y (2006) Tissue-engineered bone repair of goat-femur defects with osteogenically induced bone marrow stromal cells. Tissue Eng 12:423
40. Pluhar GE, Turner AS, Pierce AR, Toth CA, Wheeler DL (2006) A comparison of two biomaterial carriers for osteogenic protein-1 (BMP-7) in an ovine critical defect model. J Bone Joint Surg Br 88:960–966
41. Fialkov JA, Holy CE, Shoichet MS, Davies JE (2003) In vivo bone engineering in a rabbit femur. J Craniofac Surg 14:324–332
42. Fan JJ, Mu TW, Qin JJ, Bi L, Pei GX (2015) Different effects of implanting sensory nerve or blood vessel on the vascularization, neurotization, and osteogenesis of tissue-engineered bone in vivo. Biomed Res Int 2014:412570
43. Nimrod R, Tova B, Alon B, Ben S, Michal ST, Yankel G et al (2009) Transplanted blood-derived endothelial progenitor cells (EPC) enhance bridging of sheep tibia critical size defects. Bone 45:918–924
44. Boyde A, Corsi A, Quarto R, Cancedda R, Bianco P (1999) Osteoconduction in large macroporous hydroxyapatite ceramic implants: evidence for a complementary integration and disintegration mechanism. Bone 24:579–589
45. Oryan A, Alidadi S, Bigham-Sadegh A, Moshiri A (2016) Comparative study on the role of gelatin, chitosan and their combination as tissue engineered scaffolds on healing and regeneration of critical sized bone defects: an in vivo study. J Mater Sci Mater Med 27:155
46. Shafiei Z, Bigham AS, Dehghani SN, Nezhad ST (2009) Fresh cortical autograft versus fresh cortical allograft effects on experimental bone healing in rabbits: radiological, histopathological and biomechanical evaluation. Cell Tissue Bank 10:19–26
47. Dehghani SN, Bigham AS, Nezhad ST, Shafiei Z (2008) Effect of bovine fetal growth plate as a new xenograft in experimental bone defect healing: radiological, histopathological and biomechanical evaluation. Cell Tissue Bank 9:91–99
48. Itoi T, Harada Y, Irie H, Sakamoto M, Tamura K, Yogo T et al (2016) Escherichia coli-derived recombinant human bone morphogenetic protein-2 combined with bone marrow-derived mesenchymal stromal cells improves bone regeneration in canine segmental ulnar defects. BMC Vet Res 12:201
49. Bigham AS, Dehghani SN, Shafiei Z, Nezhad ST (2008) Xenogenic demineralized bone matrix and fresh autogenous cortical bone effects on experimental bone healing: radiological, histopathological and biomechanical evaluation. J Orthop Traumatol 9:73–80
50. Kimelman-Bleich N, Pelled G, Zilberman Y, Kallai I, Mizrahi O, Tawackoli W et al (2011) Targeted gene-and-host progenitor cell therapy for nonunion bone fracture repair. Mol Ther 19:53
51. Kimelman BN, Pelled GD (2009) The use of a synthetic oxygen carrier-enriched hydrogel to enhance mesenchymal stem cell-based bone formation in vivo. Biomaterials 30:4639–4648
52. Sun JS, Chen PY, Tsuang YH, Chen MH, Chen PQ (2009) Vitamin-D binding protein does not enhance healing in rat bone defects: a pilot study. Clin Orthop Relat Res 467:3156–3164
53. Lazard ZW, Heggeness MH, Hipp JA, Corinne S, Fuentes AS, Nistal RP et al (2011) Cell-based gene therapy for repair of critical size defects in the rat fibula. J Cell Biochem 112:1563–1571
54. Chakkalakal D, Strates B, Garvin K, Novak J, Fritz E, Mollner T et al (2001) Demineralized bone matrix as a biological scaffold for bone repair. Tissue Eng 7:161–177

55. Shafiei-Sarvestani Z, Oryan A, Bigham AS, Meimandi-Parizi A (2012) The effect of hydroxyapatite-hPRP, and coral-hPRP on bone healing in rabbits: radiological, biomechanical, macroscopic and histopathologic evaluation. Int J Surg 10:96–101
56. Oryan A, Meimandi PA, Shafieisarvestani Z, Bigham AS (2012) Effects of combined hydroxyapatite and human platelet rich plasma on bone healing in rabbit model: radiological, macroscopical, histopathological and biomechanical evaluation. Cell Tissue Bank 13:639–651
57. Bigham-Sadegh A, Karimi I, Shadkhast M, Mahdavi MH (2015) Hydroxyapatite and demineralized calf fetal growth plate effects on bone healing in rabbit model. J Orthop Traumatol 16:141–149
58. Zellin G, Linde A (1997) Treatment of segmental defects in long bones using osteopromotive membranes and recombinant human bone morphogenetic protein-2: an experimental study in rabbits. Scand J Plast Reconstr Surg Hand Surg 31:97–104
59. Luca L, Rougemont AL, Walpoth BH, Boure L, Tami A, Anderson JM et al (2015) Injectable rhBMP-2-loaded chitosan hydrogel composite: osteoinduction at ectopic site and in segmental long bone defect. J Biomed Mater Res A 96A:66–74
60. Tu J, Wang H, Li H, Dai K, Wang J, Zhang X (2009) The in vivo bone formation by mesenchymal stem cells in zein scaffolds. Biomaterials 30:4369–4376
61. Satoshi K, Ryuhei F, Shoji Y, Shinji F, Kazutoshi N, Koichiro T et al (2003) Bone regeneration by recombinant human bone morphogenetic protein-2 and a novel biodegradable carrier in a rabbit ulnar defect model. Biomaterials 24:1643–1651
62. Bostrom M, Lane JM, Tomin E, Browne M, Berberian W, Turek T et al (1996) Use of bone morphogenetic protein-2 in the rabbit ulnar nonunion model. Clin Orthop Relat Res 327:272–282
63. Bouxsein ML, Turek TJ, Blake CA, D'Augusta D, Li X, Stevens M et al (2001) Recombinant human bone morphogenetic protein-2 accelerates healing in a rabbit ulnar osteotomy model. J Bone Joint Surg Am 83-A:1219
64. Geuze RE, Theyse LFH, Kempen DHR, Hazewinkel HAW, Kraak HYA, Oner FC et al (2012) A differential effect of bone morphogenetic protein-2 and vascular endothelial growth factor release timing on osteogenesis at ectopic and orthotopic sites in a large-animal model. Tissue Eng Part A 18:2052–2062
65. Theyse LF, Oosterlaken-Dijksterhuis MA, Van DJ, Dhert WJ, Hazewinkel HA (2006) Growth hormone stimulates bone healing in a critical-sized bone defect model. Clin Orthop Relat Res 446:259
66. Jones CB, Sabatino CT, Badura JM, Sietsema DL, Marotta JS (2008) Improved healing efficacy in canine ulnar segmental defects with increasing recombinant human bone morphogenetic protein-2/allograft ratios. J Orthop Trauma 22:550–559
67. Cook SD, Baffes GC, Wolfe MW, Sampath TK, Rueger DC (1994) Recombinant human bone morphogenetic protein-7 induces healing in a canine long-bone segmental defect model. Clin Orthop Relat Res 301:302
68. Bigham-Sadegh A, Mirshokraei P, Karimi I, Oryan A, Aparviz A, Shafiei-Sarvestani Z (2012) Effects of adipose tissue stem cell concurrent with greater omentum on experimental long-bone healing in dog. Connect Tissue Res 53:334–342
69. Zhang X, Zhu L, Cao Y, Liu Y, Xu Y, Ye W et al (2012) Repair of rabbit femoral condyle bone defects with injectable nanohydroxyapatite/chitosan composites. J Mater Sci Mater Med 23:1941–1949
70. Kanazawa M, Tsuru K, Fukuda N, Sakemi Y, Nakashima Y, Ishikawa K (2017) Evaluation of carbonate apatite blocks fabricated from dicalcium phosphate dihydrate blocks for reconstruction of rabbit femoral and tibial defects. J Mater Sci Mater Med 28:85
71. Betti LV, Bramante PCM, Cestari PTM, Granjeiro PJM, Garcia PRB (2011) Repair of rabbit femur defects with organic bovine bone cancellous block or cortical granules. Int J Oral Maxillofac Implants 26:1167
72. Gil-Albarova J, Vila M, Badiola-Vargas J, Sánchez-Salcedo S, Herrera A, Vallet-Regi M (2012) In vivo osteointegration of three-dimensional crosslinked gelatin-coated hydroxyapatite foams. Acta Biomater 8:3777–3783

73. Zheng H, Bai Y, Shih MS, Hoffmann C, Peters F, Waldner C et al (2014) Effect of a β-TCP collagen composite bone substitute on healing of drilled bone voids in the distal femoral condyle of rabbits. J Biomed Mater Res B Appl Biomater 102:376–383
74. Liu J, Mao K, Liu Z, Wang X, Cui F, Guo W et al (2013) Injectable biocomposites for bone healing in rabbit femoral condyle defects. PLoS One 8:e75668
75. Alireza RG, Lambers FM, Mehdi GR, Ralph M, Pioletti DP (2011) In vivo loading increases mechanical properties of scaffold by affecting bone formation and bone resorption rates. Bone 49:1357–1364
76. Guihard P, Boutet MA, Brounais-Le Royer B, Gamblin AL, Amiaud J, Renaud A et al (2015) Oncostatin m, an inflammatory cytokine produced by macrophages, supports intramembranous bone healing in a mouse model of tibia injury. Am J Pathol 185:765–775
77. Laurent M, Bénédicte R, Olivier C, Jean-Christophe F (2010) Drilled hole defects in mouse femur as models of intramembranous cortical and cancellous bone regeneration. Calcif Tissue Int 86:72–81
78. Nagashima M, Sakai A, Uchida S, Tanaka S, Tanaka M, Nakamura T (2005) Bisphosphonate (YM529) delays the repair of cortical bone defect after drill-hole injury by reducing terminal differentiation of osteoblasts in the mouse femur. Bone 36:502–511
79. Xu W, Ganz C, Weber U, Adam M, Holzhüter G, Wolter D et al (2011) Evaluation of injectable silica-embedded nanohydroxyapatite bone substitute in a rat tibia defect model. Int J Nanomedicine 2011:1543–1552
80. Trejo CG, Lozano D, Manzano M, Doadrio JC, Salinas AJ, Dapía S et al (2010) The osteoinductive properties of mesoporous silicate coated with osteostatin in a rabbit femur cavity defect model. Biomaterials 31:8564–8573
81. Guillemin G, Patat JL, Fournie J, Chetail M (2010) The use of coral as a bone graft substitute. J Biomed Mater Res A 21:557–567
82. Choi S, Liu IL, Yamamoto K, Honnami M, Sakai T, Ohba S et al (2014) Implantation of tetrapod-shaped granular artificial bones or Î²-tricalcium phosphate granules in a canine large bone-defect model. J Vet Med Sci 76:229–235
83. Smit TH (2002) The use of a quadruped as an in vivo model for the study of the spine—biomechanical considerations. Eur Spine J 11:137–144
84. Bloemers FW, Stahl JP, Sarkar MR, Linhart W, Rueckert U, Wippermann BW (2004) Bone substitution and augmentation in trauma surgery with a resorbable calcium phosphate bone cement. Eur J Trauma 30:17–22
85. Liang H, Wang K, Shimer AL, Li X, Balian G, Shen FH (2010) Use of a bioactive scaffold for the repair of bone defects in a novel reproducible vertebral body defect model. Bone 47:197–204
86. Dmitriy S, Ilan K, Wafa T, Doron CY, Anthony O, Susan S et al (2011) Gene-modified adult stem cells regenerate vertebral bone defect in a rat model. Mol Pharm 8:1592
87. Quan R, Ni Y, Zhang L, Xu J, Zheng X, Yang D (2014) Short- and long-term effects of vertebroplastic bone cement on cancellous bone. J Mech Behav Biomed Mater 35:102–110
88. Yang HL, Zhu XS, Chen L, Chen CM, Mangham DC, Coulton LA et al (2012) Bone healing response to a synthetic calcium sulfate/β-tricalcium phosphate graft material in a sheep vertebral body defect model. J Biomed Mater Res B Appl Biomater 100B:1911–1921
89. Zhu X, Chen X, Chen C, Wang G, Gu Y, Geng D et al (2012) Evaluation of calcium phosphate and calcium sulfate as injectable bone cements in sheep vertebrae. J Spinal Disord Tech 25:333
90. Kobayashi H, Turner AS, Kawamoto T, Bauer TW (2010) Evaluation of a silica-containing bone graft substitute in a vertebral defect model. J Biomed Mater Res A 92A:596–603
91. Kobayashi H, Fujishiro T, Belkoff SM, Kobayashi N, Turner AS, Seim HB et al (2010) Long-term evaluation of a calcium phosphate bone cement with carboxymethyl cellulose in a vertebral defect model. J Biomed Mater Res A 88A:880–888
92. Zhen W, Bin L, Lei C, Jiang C (2011) Evaluation of an osteostimulative putty in the sheep spine. J Mater Sci Mater Med 22:185–191

93. James AW, Chiang M, Asatrian G, Shen J, Goyal R, Chung CG et al (2016) Vertebral implantation of NELL-1 enhances bone formation in an osteoporotic sheep model. Tissue Eng Part A 22:840
94. Verron E, Pissonnier ML, Lesoeur J, Schnitzler V, Fellah BH, Pascal-Moussellard H et al (2014) Vertebroplasty using bisphosphonate-loaded calcium phosphate cement in a standardized vertebral body bone defect in an osteoporotic sheep model. Acta Biomater 10:4887–4895
95. Turner TM, Urban RM, Singh K, Hall DJ, Renner SM, Lim TH et al (2008) Vertebroplasty comparing injectable calcium phosphate cement compared with polymethylmethacrylate in a unique canine vertebral body large defect model. Spine J 8:482–487
96. Manrique E, Chaparro D, Cebrián JL, López-Durán L (2014) In vivo tricalcium phosphate, bone morphogenetic protein and autologous bone marrow biomechanical enhancement in vertebral fractures in a porcine model. Int Orthop 38:1993–1999
97. Pelled G, Sheyn D, Tawackoli W, Jun DS, Koh Y, Su S et al (2016) BMP6-engineered MSCs induce vertebral bone repair in a pig model: a pilot study. Stem Cells Int 2016:1–8
98. Reichert JC, Saifzadeh S, Wullschleger ME, Epari DR, Schutz MA, Duda GN et al (2009) The challenge of establishing preclinical models for segmental bone defect research. Biomaterials 30:2149–2163
99. Vaněček V, Klíma K, Kohout A, Foltán R, Jiroušek O, Šedý J et al (2013) The combination of mesenchymal stem cells and a bone scaffold in the treatment of vertebral body defects. Eur Spine J 22:2777–2786
100. Alt V, Thormann U, Ray S, Zahner D, Dürselen L, Lips K et al (2013) A new metaphyseal bone defect model in osteoporotic rats to study biomaterials for the enhancement of bone healing in osteoporotic fractures. Acta Biomater 9:7035–7042
101. Yuan H, Li Y, de Bruijn JD, de Groot K, Zhang X (2000) Tissue responses of calcium phosphate cement: a study in dogs. Biomaterials 21:1283–1290
102. Luangphakdy V, Shinohara K, Pan H, Boehm C, Samaranska A, Muschler GF (2015) Evaluation of rhBMP-2/collagen/TCP-HA bone graft with and without bone marrow cells in the canine femoral multi defect model. Eur Cell Mater 29:57–68
103. Caralla T, Joshi P, Fleury S, Luangphakdy V, Shinohara K, Pan H et al (2013) In vivo transplantation of autogenous marrow-derived cells following rapid intraoperative magnetic separation based on hyaluronan to augment bone regeneration. Tissue Eng Part A 19:125–134
104. Luangphakdy V, Walker E, Shinohara K, Pan H, Hefferan T, Bauer TW et al (2013) Evaluation of osteoconductive scaffolds in the canine femoral multi-defect model. Tissue Eng Part A 19:634–648
105. Takigami H, Kumagai K, Latson L, Togawa D, Bauer T, Powell K et al (2010) Bone formation following OP-1 implantation is improved by addition of autogenous bone marrow cells in a canine femur defect model. J Orthop Res 25:1333–1342
106. Bigham-Sadegh A, Karimi I, Alebouye M, Shafie-Sarvestani Z, Oryan A (2013) Evaluation of bone healing in canine tibial defects filled with cortical autograft, commercial-DBM, calf fetal DBM, omentum and omentum-calf fetal DBM. J Vet Sci 14:337
107. Schubert T, Lafont S, Beaurin G, Grisay G, Behets C, Gianello P et al (2013) Critical size bone defect reconstruction by an autologous 3D osteogenic-like tissue derived from differentiated adipose MSCs. Biomaterials 34:4428–4438
108. Saifzadeh S, Pourreza B, Hobbenaghi R, Naghadeh BD, Kazemi S (2009) Autogenous greater omentum, as a free nonvascularized graft, enhances bone healing: an experimental nonunion model. J Investig Surg 22:129–137
109. Aalami OO, Nacamuli RP, Lenton KA, Cowan CM, Fang TD, Fong KD et al (2004) Applications of a mouse model of calvarial healing: differences in regenerative abilities of juveniles and adults. Plast Reconstr Surg 114:713
110. Pritzker KP, Gay S, Jimenez SA, Ostergaard K, Pelletier JP, Revell PA et al (2006) Osteoarthritis cartilage histopathology: grading and staging. Osteoarthr Cartil 14:13–29
111. Meyer RA Jr, Tsahakis PJ, Martin DF, Banks DM, Harrow ME, Kiebzak GM (2010) Age and ovariectomy impair both the normalization of mechanical properties and the accretion of mineral by the fracture callus in rats. J Orthop Res 19:428–435

112. Hae-Ryong S, Ajay P, Jeong-Hee L, Hyung-Bin P, Do-Kyung R, Gon-Sup K et al (2002) Spontaneous bone regeneration in surgically induced bone defects in young rabbits. J Pediatr Orthop B 11:343–349
113. Nagai N, Qin CL, Nagatsuka H, Inoue M, Ishiwari Y, Nagai N et al (1999) Age effects on ectopic bone formation induced by purified bone morphogenetic protein. Int J Oral Maxillofac Surg 7:107–114
114. Bosch C, Melsen B, Vargervik K (1998) Importance of the critical-size bone defect in testing bone-regenerating materials. J Craniofac Surg 9:310–316
115. Takagi K, Urist MR (1982) The reaction of the dura to bone morphogenetic protein (BMP) in repair of skull defects. Ann Surg 196:100
116. Rivas R, Shapiro F (2002) Structural stages in the development of the long bones and epiphyses: a study in the New Zealand white rabbit. J Bone Joint Surg Am 84-A:85
117. Meyer RA Jr, Meyer MH, Tenholder M, Wondracek S, Wasserman R, Garges P (2003) Gene expression in older rats with delayed union of femoral fractures. J Bone Joint Surg Am 85:1243–1254
118. Holstein JH, Garcia P, Histing T, Kristen A, Scheuer C, Menger MD et al (2008) Advances in the establishment of defined mouse models for the study of fracture healing and bone regeneration. J Orthop Trauma 23:S31–S38
119. Batten RL (1982) Bone repair and fracture healing in man. Injury 13:532–533
120. Bostrom MP, Lane JM, Berberian WS, Missri AA, Tomin E, Weiland A et al (1995) Immunolocalization and expression of bone morphogenetic proteins 2 and 4 in fracture healing. J Orthop Res 13:357
121. Kawaguchi H, Kurokawa T, Hanada K, Hiyama Y, Tamura M, Ogata E et al (1994) Stimulation of fracture repair by recombinant human basic fibroblast growth factor in normal and streptozotocin-diabetic rats. Endocrinology 135:774–781
122. Kilborn SH, Trudel G, Uhthoff HK (2002) Review of growth plate closure compared with age at sexual maturity and lifespan in laboratory animals. Contemp Top Lab Anim Sci 41:21
123. Boutrand JP (2012) Chapter 12-Methods and interpretation of performance studies for bone implants. In: Boutrand J-P (ed) Woodhead publishing series in biomaterials, biocompatibility and performance of medical devices. Woodhead Publishing, Sawston, pp 271–307. ISBN 9780857090706
124. Wang X, Mabrey JD, Agrawal CM (1998) An interspecies comparison of bone fracture properties. Biomed Mater Eng 8:1–9
125. Martiniaková M, Omelka R, Chrenek P, Ryban L, Parkányi V, Grosskopf B et al (2005) Changes of femoral bone tissue microstructure in transgenic rabbits. Folia Biol 51:140–144
126. Muschler GF, Raut VP, Patterson TE, Wenke JC, Hollinger JO (2010) The design and use of animal models for translational research in bone tissue engineering and regenerative medicine. Tissue Eng Part B Rev 16:123–145
127. Castañeda S, Largo R, Calvo E, Rodríguez-Salvanés F, Marcos ME, Díaz-Curiel M et al (2006) Bone mineral measurements of subchondral and trabecular bone in healthy and osteoporotic rabbits. Skelet Radiol 35:34–41
128. Newman E, Turner AS, Wark JD (1995) The potential of sheep for the study of osteopenia: current status and comparison with other animal models. Bone 16:277S
129. Gilsanz V, Roe TF, Gibbens DT, Schulz EE, Carlson ME, Gonzalez O et al (1988) Effect of sex steroids on peak bone density of growing rabbits. Am J Physiol 255:E416–EE21
130. Viateau V, Guillemin G (2005) Experimental animal models for tissue-engineered bone regeneration In: Quarto R, Petite H (Eds) Engineered bone (pp 89–104). Austin: Landes Bioscience
131. Aerssens J, Boonen S, Lowet G, Dequeker J (1998) Interspecies differences in bone composition, density, and quality: potential implications for in vivo bone research. Endocrinology 139:663–670
132. Gong JK, Arnold JS, Cohn SH (1964) Composition of trabecular and cortical bone. Anat Rec 149:325–331
133. Stover BJ, Andersen AC (1971) The beagle as an experimental dog. Radiat Res 45:449

134. Kimmel DB, Jee WS (2010) A quantitative histologic study of bone turnover in young adult beagles. Anat Rec 203:31–45
135. Fernández-Tresguerres-Hernández-Gil I, Alobera-Gracia MA, Del-Canto-Pingarrón M, Blanco-Jerez L (2006) Physiological bases of bone regeneration I. Histology and physiology of bone tissue. Med Oral Patol Oral Cir Buca 11:E47–E51
136. Anderson M, Dhert BJ, Dalmeijer R, Leenders H, Van BC, Verbout A (1999) Critical size defect in the goat's os ilium. A model to evaluate bone grafts and substitutes. Clin Orthop Relat Res 364:231
137. Van Der Donk S, Buma P, Aspenberg P, Schreurs BW (2001) Similarity of bone ingrowth in rats and goats: a bone chamber study. Comp Med 51:336
138. Eitel F, Klapp F, Jacobson W, Schweiberer L (1981) Bone regeneration in animals and in man. A contribution to understanding the relative value of animal experiments to human pathophysiology. Arch Orthop Trauma Surg 99(1):59–64
139. Liebschner MAK (2004) Biomechanical considerations of animal models used in tissue engineering of bone. Biomaterials 25:1697–1714
140. Qin L, Mak AT, Cheng CW, Hung LK, Chan KM (2010) Histomorphological study on pattern of fluid movement in cortical bone in goats. Anat Rec Adv Integr Anat Evol Biol 255:380–387
141. Turner AS, Villanueva AR (1994) Static and dynamic histomorphometric data in 9- to 11-year-old ewes. Vet Comp Orthop Traumatol 07:101–109
142. Den Boer FC, Patka P, Bakker FC, Wippermann BW, Lingen A, Van VGQ et al (2010) New segmental long bone defect model in sheep: quantitative analysis of healing with dual energy x-ray absorptiometry. J Orthop Res 17:654–660
143. Spaargaren DH (1994) Metabolic rate and body size: a new view on the 'surface law' for basic metabolic rate. Acta Biotheor 42:263
144. Willie BM, Bloebaum RD, Bireley WR (2010) Determining relevance of a weight-bearing ovine model for bone ingrowth assessment. J Biomed Mater Res A 69(3):567–576
145. Lamerigts NM, Buma P, Huiskes R, Schreurs W, Gardeniers J, Slooff TJ (2000) Incorporation of morsellized bone graft under controlled loading conditions. A new animal model in the goat. Biomaterials 21:741–747
146. Raschke M, Kolbeck S, Bail H, Schmidmaier G, Flyvbjerg A, Lindner T et al (2001) Homologous growth hormone accelerates healing of segmental bone defects. Bone 29:368–373
147. Michael T, Stefan SM, Peter K, Joerg W, Karl Andreas S (2005) Bone regeneration in osseous defects using a resorbable nanoparticular hydroxyapatite. J Oral Maxillofac Surg 63:1626–1633
148. Raab DM, Crenshaw TD, Kimmel DB, Smith EL (2010) A histomorphometric study of cortical bone activity during increased weight-bearing exercise. J Bone Miner Res 6:741–749
149. Ermanno B, Paola B (2014) Osteoporosis-bone remodeling and animal models. Toxicol Pathol 42:957–969
150. Mosekilde L, Kragstrup J, Richards A (1987) Compressive strength, ash weight, and volume of vertebral trabecular bone in experimental fluorosis in pigs. Calcif Tissue Int 40:318–322
151. Li M, Weisbrode SE, Safron JA, Stills HG, Jankowsky ML, Ebert DC et al (1992) Calcium-restricted ovariectomized sinclair s-1 minipigs: an animal model of osteopenia and trabecular plate perforation. Bone 13:379
152. Kragstrup J, Richards A, Fejerskov O (1989) Effects of fluoride on cortical bone remodeling in the growing domestic pig. Bone 10:421–424
153. Swindle MM, Smith AC, Hepburn BJ (1988) Swine as models in experimental surgery. J Investig Surg 1:65–79
154. O'Loughlin PF, Morr S, Bogunovic L, Kim AD, Park B, Lane JM (2008) Selection and development of preclinical models in fracture-healing research. J Bone Joint Surg Am 90(Suppl 1):79–84
155. Martini L, Fini M, Giavaresi G, Giardino R (2001) Sheep model in orthopedic research: a literature review. Comp Med 51:292–299

156. Paige KT, Cima LG, Yaremchuk MJ, Vacanti JP, Vacanti CA (1995) Injectable cartilage. Plast Reconstr Surg 96:1390–1398
157. Jackson RW, Reed CA, Israel JA, Abou-Keer FK, Garside H (1970) Production of a standard experimental fracture. Can J Surg 13:415–420
158. Bonnarens F, Einhorn TA (1984) Production of a standard closed fracture in laboratory animal bone. J Orthop Res 2:97–101
159. Marturano J, Cleveland BC, Byrne MA, O'Connell S, Wixted J, Billiar K (2008) An improved murine femur fracture device for bone healing studies. J Biomech 41:1222–1228
160. Hebb JH, Ashley JW, Mcdaniel L, Lopas LA, Tobias J, Hankenson KD et al (2018) Bone healing in an aged murine fracture model is characterized by sustained callus inflammation and decreased cell proliferation. J Orthop Res 36(1):149–158
161. Lopas LA, Belkin NS, Mutyaba PL, Gray CF, Hankenson KD, Jaimo A (2014) Fractures in geriatric mice show decreased callus expansion and bone volume. Clin Orthop Relat Res 472:3523–3532
162. Dishowitz MI, Terkhorn SP, Bostic SA, Hankenson KD (2011) Notch signaling components are upregulated during both endochondral and intramembranous bone regeneration. J Orthop Res 30:296–303
163. Puolakkainen T, Rummukainen P, Lehto J, Ritvos O, Hiltunen A, Säämänen AM et al (2017) Soluble activin type IIB receptor improves fracture healing in a closed tibial fracture mouse model. PLoS One 12:e0180593
164. Holstein JH, Menger MD, Culemann U, Meier C, Pohlemann T (2007) Development of a locking femur nail for mice. J Biomech 40:215–219
165. Manigrasso MB, O'Connor JP (2004) Characterization of a closed femur fracture model in mice. J Orthop Trauma 18:687–695
166. Thompson Z, Miclau T, Hu D, Helms JA (2010) A model for intramembranous ossification during fracture healing. J Orthop Res 20:1091–1098
167. Makino T, Hak DJ, Hazelwood SJ, Curtiss S, Reddi AH (2010) Prevention of atrophic nonunion development by recombinant human bone morphogenetic protein-7. J Orthop Res 23:632–638
168. Kumabe Y, Sang YL, Waki T, Iwakura T, Takahara S, Arakura M et al (2017) Triweekly administration of parathyroid hormone (1–34) accelerates bone healing in a rat refractory fracture model. BMC Musculoskelet Disord 18:545
169. Kokubu T, Hak DJ, Hazelwood SJ, Reddi AH (2010) Development of an atrophic nonunion model and comparison to a closed healing fracture in rat femur. J Orthop Res 21:503–510
170. Hietaniemi K, Peltonen J, Paavolainen P (1995) An experimental model for non-union in rats. Injury 26:681–686